CHAPTER 5

Study on the barrier properties and interfacial properties of self-assembled monolayers (SAMs) of aliphatic, aromatic and alkoxycyanobiphenyl thiols on gold surface prepared using a lyotropic liquid crystalline phase as an adsorbing medium

This chapter describes about a novel method of formation of self-assembled monolayers of some thiol molecules using a new hexagonal liquid crystalline phase as an adsorbing medium. It will be shown that this method has some distinct advantages over the conventional methods used for the SAM preparation. The hexagonal liquid crystalline phase consisting of water and Triton X-100 at a particular composition. For monolayer preparation, the corresponding thiol was added to this phase and used as an adsorbing medium. The phase characteristics of the hexagonal liquid crystalline phase were investigated using polarizing light microscopy (for textural studies) and X-ray diffraction (XRD) studies. It is found that the hexagonal structure of the phase is maintained even after the addition of thiol molecules. We have studied the monolayer formation of some aliphatic, aromatic and alkoxycyanobiphenyl thiol molecules using the above-mentioned hexagonal liquid crystalline phase as an adsorbing medium. The barrier properties and interfacial properties of these monolayers were evaluated and characterized using electrochemical and spectroscopic techniques. The electrochemical techniques such as cyclic voltammetry and electrochemical impedance spectroscopy were extensively used in this work. For comparison, we have also studied the monolayer

formation and characterization of the corresponding thiol molecules using organic solvents such as ethanol and dichloromethane as an adsorbing medium. This chapter has been divided into three parts. The first part deals with the monolayer formation and evaluation of its barrier properties of aliphatic thiols on gold surface using the hexagonal liquid crystalline phase as an adsorbing medium. The second and third parts contain the study of monolayers of aromatic and alkoxycyanobiphenyl thiol molecules on gold surface respectively using the above-mentioned lyotropic hexagonal liquid crystalline phase as an adsorbing medium.

I. SAMs OF ALIPHATIC THIOLS ON GOLD SURFACE

5.1. Introduction

Self assembled monolayer (SAM) refers to a single layer of molecules on various metallic and non-metallic surfaces formed by the spontaneous chemisorption leading to the formation of a highly crystalline, defect free structure with high degree of orientation, molecular ordering and packing density [1-3]. The structural and chemical properties of SAMs with ultra low defects make them interesting systems for potential applications in a variety of fields such as sensors [4-6], corrosion inhibition [7-9], photolithography [10,11], molecular wire and molecular electronics [12-14], molecular capacitors [15], high density memory storage devices [16], friction [17], wetting [18] and as a barrier for electron transfer reactions [19]. Even though the adsorption of several functional groups on different metal and non-metallic surfaces have been reported in literature, it is the SAM of n-alkanethiols on gold that is the most widely studied system owing to the flexibility offered by the aliphatic chains, the inertness of gold surface and the ease of preparation by a simple immersion process [20]. The SAMs of aliphatic thiols are usually obtained by

immersing the metal into a dilute organic solution containing the thiol molecule whose concentration varies from typically μM to mM in solvents such as ethanol and acetonitrile. Based on the measurement of interfacial capacitance of alkanethiol SAMs on gold surface adsorbed from different non-aqueous solvents, it has been shown by Sur and Lakshminarayanan [21,22] that the permeability of these SAMs largely depends on the solvent used for adsorption and the blocking properties of these monolayers have been correlated to the bulk structure of the corresponding solvent used for the adsorption. Usually the barrier property of the SAM is evaluated by electrochemical techniques such as cyclic voltammetry and impedance spectroscopy using the redox probes like potassium ferro/ferri cyanide and hexaammineruthenium(III) chloride [23-25]. However, as far as the commercial applications of SAM are concerned, the use of organic solvents is a major drawback due to their volatility and toxicity. Besides, the intercalation of the solvent molecules within the monolayer during the process of adsorption is a major problem in obtaining a compact and defect free SAM.

Surface-active agents, often known as surfactants can also form the self-assembled structures such as micelles and reverse micelles in aqueous solutions that can generate the hydrophobic domains that can solvate and solubilize the non-polar species [26]. The solvating ability of these self-assembled structures depends on the nature of the surfactant, the temperature and the additives. By changing the concentration of the surfactant and/or water, we can generate various structures including that of different liquid crystalline phases such as hexagonal, reverse hexagonal and lamellar phases. In this paper, we have used for the first time a lyotropic hexagonal liquid crystalline phase consisting of water and a commonly used non-ionic surfactant, Triton X-100

(poly(ethylene glycol)-tert-octylphenylether) [27] for the preparation of monolayer.

We find from literature that there are some reports on the formation of self-assembled monolayers of aliphatic thiols from aqueous micellar solutions of various surfactants. Miller et al. reported that the rate of formation of monolayer of hydroxyl-terminated n-alkanethiols is enhanced in the presence of micelles of decyltrimethylammonium bromide in aqueous solution [28]. Liu and Kaifer prepared the SAMs of dodecanethiol from aqueous micellar solutions of Triton X-100, sodium dodecyl sulphate and hexadecyltrimethylammonium bromide and found that the rate of formation of the monolayer increases with increasing surfactant concentration above the critical micellar concentration (CMC) [29]. These authors attributed this effect to the presence of large number of micelles at higher surfactant concentration enhancing the solubilization of thiol in the hydrophobic core. Jennings et al. have extensively studied the preparation and stability of SAMs using aqueous micellar solutions [30-33]. Yan et al. reported the formation of SAMs of n-alkanethiolates on gold from aqueous micellar solutions of non-ionic poly-(oxyethylene) monododecyl ethers and found greater enhancement in the overall chain densities than the SAMs obtained from the traditional organic solvents such as ethanol [30]. Consistent with a more defect free structure, these water-borne SAMs exhibit higher resistances against the diffusion of redox probes. These authors also reported the formation of SAM of hexadecanethiol on gold from aqueous micellar solution of $C_{12}E_6$ and found that the monolayer so formed is highly compact and dense, showing good barrier property towards the redox probes [31]. Jennings et al. [32] investigated the formation of SAMs of n-alkanethiols on gold from aqueous micellar solutions of n-alkyltrimethylammonium bromides and proposed a mechanism for the self-

assembly of thiols on gold in micellar solutions. Apart from the preparation and stability, Jennings et al. also studied the kinetics of monolayer formation in micelles and reported that the initial step follows a first order Langmuir adsorption model, which is slower compared to the rate of the initial step in ethanol solution [31, 33]. To the best of our knowledge, there is no report in literature on the formation and characterization of SAMs using hexagonal lyotropic liquid crystalline phase as an adsorbing medium.

In this chapter, we have discussed about the preparation and characterization of self assembled monolayers of decanethiol and hexadecanethiol on gold surface using a hexagonal lyotropic liquid crystalline phase as an adsorbing medium and we have also compared our results with that of the corresponding SAMs obtained using ethanol as a solvent. The hexagonal structure of the liquid crystalline phase consisting of water, Triton X-100 and the corresponding thiol, is confirmed by polarizing light microscopy and X-ray diffraction (XRD) studies. Among several techniques used for characterization of SAM, the electrochemical methods are most effective in assessing the quality of the monolayer film. We have used electrochemical techniques such as cyclic voltammetry and impedance spectroscopy to evaluate the barrier properties and insulating properties of the SAMs using potassium ferro/ferri cyanide and hexaammineruthenium(III) chloride as redox probe molecules. Impedance spectroscopy data were used to determine the capacitance, ionic permeability, surface coverage and other kinetic parameters of the SAM modified electrodes. We have also carried out grazing angle FTIR spectroscopy studies to characterize the orientation and packing of these SAMs on Au surface. In addition to the ease of formation and environmental benefits associated with the aqueous solvents, the method described here for preparing the monolayer

produces a highly compact and almost defect free structure, which is crucial in the applications and commercial development of devices based on SAM.

5.2. Experimental section

5.2.1. Chemicals

All the chemical reagents used in this work were analytical grade (AR) reagents. Decanethiol (Aldrich), Hexadecanethiol (Aldrich), ethanol 99.95% (Merck), Triton X-100 (Spectrochem), potassium ferrocyanide (Loba), potassium ferricyanide (Qualigens), hexaammineruthenium(III) chloride (Alfa Aesar), sodium fluoride (Qualigens) and lithium perchlorate (Acros Organics) were used in this study as received. Millipore water having a resistivity of 18 MΩ cm was used to prepare the aqueous solutions.

5.2.2. Preparation of a hexagonal lyotropic liquid crystalline phase

The lyotropic liquid crystalline phase is a mixture of Triton X-100 (42% by weight) and water (58% by weight) [34], which exhibits the broken mosaic and focal conic textures of the hexagonal phase in textural studies using polarizing light microscopy. The hexagonal structure of the liquid crystalline phase is also confirmed by X-ray diffraction studies. For the preparation of SAMs, the corresponding thiol was added to the above-mentioned liquid crystalline phase. About 2ml of neat thiol was added to the total volume of 25ml of the hexagonal liquid crystalline phase. Initially, the liquid crystalline phase was heated to the isotropic phase at around 40^0C – 45^0C into which the thiol was added and stirred completely to obtain a homogeneous mixture of solution. Then it was allowed to cool down to room temperature and used for the SAM formation. Even after the addition of thiol, the hexagonal structure of

the liquid crystalline phase is maintained and it was confirmed by polarizing light microscopy and X-ray diffraction studies.

5.2.3. Sample preparation

Gold sample of purity 99.99% was obtained from Arora Mathey, India. Evaporated gold (~100 nm thickness) on glass with chromium underlayers (~ 2-5 nm thickness) was used for the monolayer formation and its characterization using electrochemical techniques and grazing angle FTIR spectroscopy. The substrate was heated to 350^0C during gold evaporation under a vacuum pressure of 2 X 10^{-5} mbar, a process that normally yields a very smooth gold substrate with predominantly Au(111) orientation. The evaporated gold samples were used as strips for SAM formation and its analysis.

For electrochemical characterization, a conventional three-electrode electrochemical cell was used. A platinum foil of large surface area was used as a counter electrode and a saturated calomel electrode (SCE) was used as a reference electrode with the SAM modified gold electrode as a working electrode. The cell was thoroughly cleaned before each experiment and kept in a hot air oven at 100^0C for at least 1 hour before the start of the experiment.

5.2.4. Preparation of SAMs from the hexagonal liquid crystalline phase

Before SAM formation, the evaporated Au strips were pre-treated with "piranha" solution (It is a mixture of 30% H_2O_2 and Conc. H_2SO_4 in 1:3 ratio) and washed completely with millipore water. The monolayers of decanethiol and hexadecanethiol were prepared by keeping the Au strips in the hexagonal liquid crystalline phase containing the thiol for about 1 hour and 15 hours at room temperature. After this, the electrode was thoroughly washed with a jet of distilled water and finally with millipore water. For comparison, we have also

prepared the monolayers of decanethiol and hexadecanethiol on Au using ethanol as a solvent. In this case, the Au strips were dipped in 1mM thiol in ethanol solution for about 1 hour and 15 hours at room temperature. Upon removal, the SAM coated electrodes were rinsed with ethanol, washed with distilled water and finally with millipore water and immediately used for the analysis.

5.2.5. Electrochemical characterization

Cyclic voltammetry and electrochemical impedance spectroscopy were used for the characterization of SAM and evaluation of its barrier property by studying the electron transfer reactions on the SAM modified surfaces using two different redox probes namely potassium ferrocyanide (negative redox probe) and hexaammineruthenium(III) chloride (positive redox probe). Cyclic voltammetry was performed in solutions of 10mM potassium ferrocyanide in 1M sodium fluoride at a potential range of –0.1V to 0.5V vs. SCE and 1mM hexaammineruthenium(III) chloride in 0.1M lithium perchlorate at a potential range of –0.4V to 0.1V vs. SCE. The impedance measurements were carried out using an ac signal of 10mV amplitude at a formal potential of the redox couple using a wide frequency range of 100kHz to 0.1Hz, in solution containing always equal concentrations of both the oxidized and reduced forms of the redox couple namely, 10mM potassium ferrocyanide and 10mM potassium ferricyanide in 1M NaF. All the experiments were performed at room temperature.

5.2.6. Instrumentation

Cyclic voltammetry was carried out using an EG&G potentiostat (model 263A) interfaced to a computer through a GPIB card (National

Instruments). The potential ranges and scan rates used are shown in the respective diagrams. For electrochemical impedance studies the potentiostat was used along with an EG&G 5210 lock-in-amplifier controlled by Power Sine software. The electrochemical impedance spectroscopy data were used for the equivalent circuit fitting analysis using Zsimpwin software (EG&G) developed on the basis of Boukamp's model. Based on this procedure, the charge transfer resistance values (R_{ct}) of SAM modified electrodes were calculated, from which the surface coverage and other kinetic parameters were also determined. In addition the impedance data were used for the pinhole analysis to evaluate the distribution of pinholes and defects present within the monolayer and to determine the surface coverage of the monolayer on Au surface.

The FTIR spectra were obtained using a FTIR 8400 model (SHIMADZU) with a fixed 85^0 grazing angle attachment (FT-85; Thermo Spectra-Tech). X-ray diffraction studies were carried out using a X-ray diffractometer (Rigaku, UltraX 18) operating at 50 kV and 80 mA using Cu Kα radiation having a wavelength of 1.54 Å.

5.3. Results and discussion

5.3.1. Polarizing light microscopy

The polarizing light microscopy is a very simple and inexpensive experimental technique, which can be used to identify the various mesophases formed by the self-assembly of surfactants. The experiments were conducted using glass slides and cover slips with the sample sandwiched between them. The textural studies were carried out by heating the sample to isotropic phase using Mettler heating arrangement and recording the textures during the process of cooling. Figure 1 shows the textures obtained for the hexagonal liquid crystalline phase system. Figure 1 (A) shows the broken focal conic texture [35]

obtained for the binary system of water and Triton X-100 without thiol. Figures 1 (B) and (C) show the similar textures and striations [36] corresponding to the hexagonal liquid crystalline phases containing in addition to Triton X-100/water, decanethiol and hexadecanethiol respectively. The phase transition from the hexagonal liquid crystalline phase to isotropic phase occurs for both the systems at a temperature above 35^0C and 45^0C respectively.

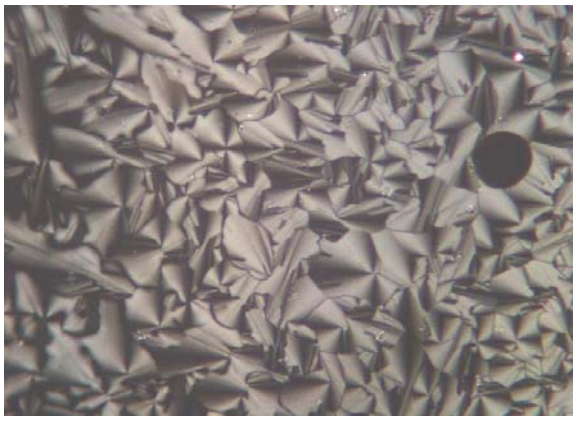

Figure 1A

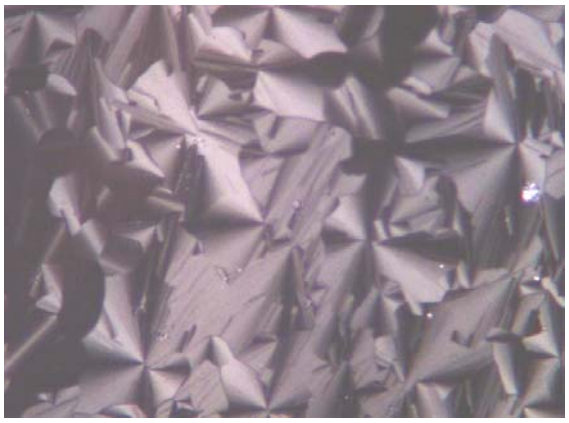

Figure 1B

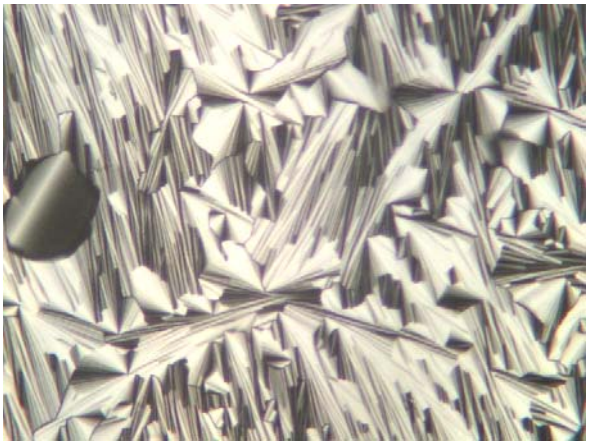

Figure 1C

Figure 1: Polarizing light microscopic textures of the hexagonal liquid crystalline phase formed by (A) Triton X-100 and water, (B) Triton X-100, water and decanethiol and (C) Triton X-100, water and hexadecanethiol at room temperature.

5.3.2. X-ray diffraction studies of the hexagonal liquid crystalline phase

The hexagonal structure of the lyotropic liquid crystalline phase is also confirmed by X-ray diffraction (XRD) studies. X-rays were produced from a rotating anode X-ray generator (Rigaku, UltraX 18) operating at 50 kV and 80 mA. The Cu Kα radiation having a wavelength of 1.54 Å was selected using a flat graphite monochromator (Huber). The sample was taken in a glass capillary (Hampton Research) having an outer diameter of 0.5mm to 1mm and a wall thickness of ~0.01mm. Then it was placed in a locally built temperature controlled heater with a stability of ± 0.1^0C. We have carried out most of our experiments at room temperature. The data were collected using an image plate (Marresearch) having a diameter of 80mm. The sample to film distance was varied from 200mm to 300mm. We have used typical exposure time of 1-2 hours for data collection. XRD images obtained for the respective systems exhibiting the hexagonal liquid crystalline phases were converted to intensity versus θ plots using the formulae.

Figure 2 shows the intensity versus θ plots and the corresponding XRD pattern for the hexagonal liquid crystalline phase containing water and Triton X-100 (A), water, Triton X-100 and decanethiol (B) and water, Triton X-100 and hexadecanethiol (C) systems respectively. It can be seen from the figure that the liquid crystalline phase shows the characteristic reflections expected for the hexagonal structure. We have calculated the 'd' spacing for all the systems using the Bragg's law and its equation and it follows the order 1 : 1/√3 : 1/√4 in all the cases showing the presence of hexagonal order in the liquid crystalline phase. The third reflection is not clear in all the systems studied in this work and it is represented by an arrow in the intensity versus θ plots, shown in the figure 2. The corresponding XRD pattern of the hexagonal liquid crystalline

phase for all the system is also shown in the lower part of the figure 2. It can be seen from the XRD patterns that the liquid crystalline phase shows three orders of reflections corresponding to the hexagonal structure of the phase. We have calculated the 'd' spacing values of 60.28Å, 71.14Å and 74.83Å for the liquid crystalline phases containing in addition to Triton X-100/water, decanethiol and hexadecanethiol respectively, using Bragg's equation. These 'd' spacing values follow the order of 1 : $1/\sqrt{3}$: $1/\sqrt{4}$, conforming the hexagonal structure of the liquid crystalline phases for all the system studied in this work. From the XRD studies, it is clear that the hexagonal structure of the liquid crystalline phase is maintained even after the addition of thiol molecules that confirms to our observations using polarizing light microscopy described earlier.

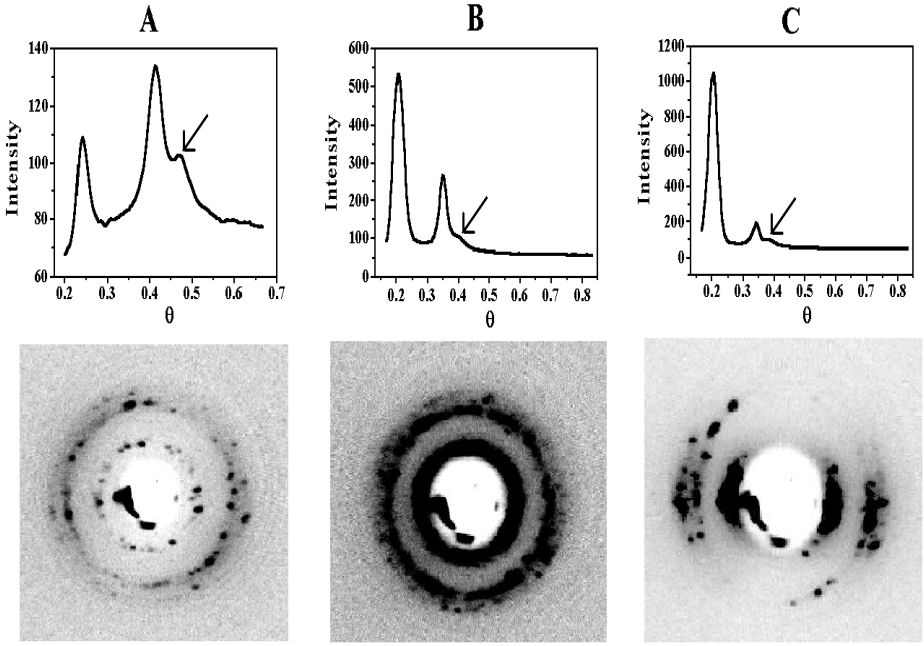

Figure 2: Intensity versus θ plots and the corresponding XRD patterns of the hexagonal liquid crystalline phase formed by (A) Triton X-100 and water, (B) Triton X-100, water and decanethiol and (C) Triton X-100, water and hexadecanethiol at room temperature.

5.3.3. Electrochemical characterization

5.3.3.1. Cyclic voltammetry

Cyclic voltammetry is an important technique to assess the quality of the monolayer and its barrier property by studying the electron transfer reaction of redox probe molecule on the SAM modified surfaces. The SAMs of decanethiol and hexadecanethiol on gold surface were formed from the hexagonal liquid crystalline phase containing the respective thiol. For comparison the corresponding monolayers obtained using ethanol as a solvent were also characterized. Figure 3A shows the cyclic voltammograms of bare Au electrode and SAM of decanethiol coated Au electrodes in 10mM potassium ferrocyanide with 1M NaF as the supporting electrolyte at a potential scan rate of 50mV/s. Similarly, Figure 3B shows the comparison of cyclic voltammograms of bare Au electrode and the monolayer of hexadecanethiol coated Au electrodes in the same solution. Insets show the cyclic voltammograms of respective SAM modified electrodes formed from ethanol and hexagonal liquid crystalline phase in the same solution. The monolayers were formed by keeping the Au strips in the corresponding thiol solution for about 15 hours. It can be seen from the figure that the bare Au electrode (Figures 3A (a) and 3B (a)) shows a perfect reversible voltammogram for the redox couple indicating that the electron transfer reaction is completely diffusion controlled. In contrast, the monolayers of decanethiol-coated electrodes (Fig. 3A (b) & (c)) do not show any peak formation as the redox reaction is completely blocked by the monolayer. Similarly, the CVs of hexadecanethiol-modified electrodes (Fig. 3B (b) & (c)) also show a good blocking behaviour indicating that the redox reaction is completely under charge transfer controlled. However, they exhibit current-voltage behaviour similar to that of a microelectrode array, as shown by the pinhole analysis

described later. It can be noted from the insets that the monolayers formed from the hexagonal liquid crystalline phase (Figures 3A (c) and 3B (c)) exhibit a more blocking characteristic than the one formed from ethanol (Figures 3A (b) and 3B (b)). The magnitude of current is almost four times lower at a positive potential range of >0.1V vs. SCE in the case of SAMs formed from the hexagonal liquid crystalline phase, when compared to the monolayers formed using ethanol as a solvent. This clearly shows that the SAMs formed from the liquid crystalline phase have a better blocking property and are highly ordered and compact with ultra-low defect density. The small current flow arises due to the access of the redox species to the gold surface through the pinholes and defects present in the monolayer.

We have also studied the cyclic voltammetric behaviour of the SAM formed in the hexagonal liquid crystalline phase and in ethanol medium by keeping the Au sample for about 1 hour. The purpose of this experiment is to evaluate the blocking ability of the SAM formed in a shorter time that will indicate the extent of adsorption and subsequent organization of the monolayer film. Figure 3C shows the CVs of the monolayer of decanethiol (about 1 hour) coated Au electrodes in 10mM potassium ferrocyanide with 1M NaF as the supporting electrolyte at a potential scan rate of 50mV/s. It can be seen from the figure that the SAM formed in ethanol (Fig. 3C (a)) shows larger currents and the CV features indicate poor blocking to redox reaction than the one formed in the hexagonal liquid crystalline phase (Fig. 3C (b)) for the same duration.

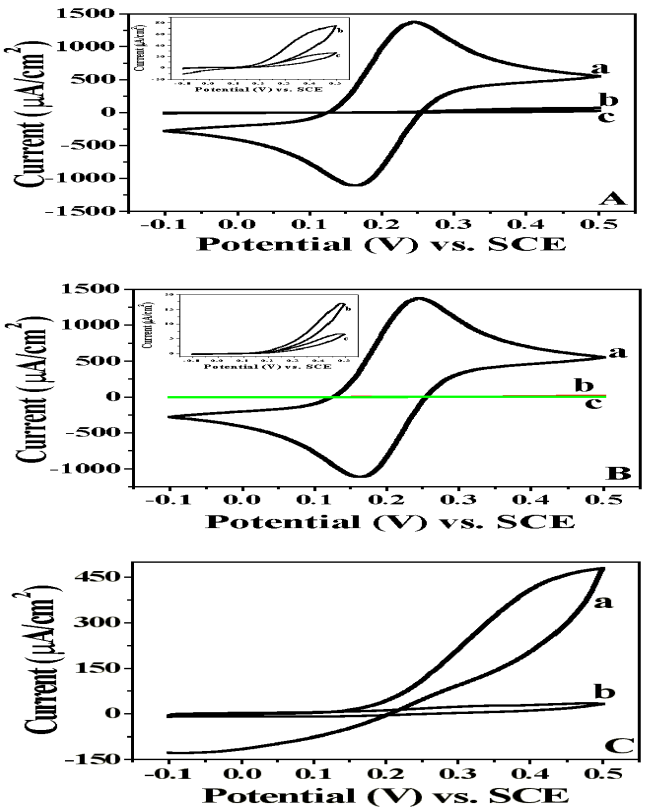

Figure 3: Cyclic voltammograms of 10mM potassium ferrocyanide with 1M NaF as supporting electrolyte at a potential scan rate of 50mV/s for, (A) Bare gold electrode (a), SAM of decanethiol formed from ethanol (b) and SAM of decanethiol formed from the hexagonal liquid crystalline phase (c) respectively for about 15hours. Inset shows the comparison of cyclic voltammograms of SAM of decanethiol formed from ethanol (b) and the hexagonal liquid crystalline phase (c). (B) Bare gold electrode (a), SAM of hexadecanethiol on Au formed from ethanol (b) and SAM of hexadecanethiol on Au formed from the hexagonal liquid phase (c) respectively for about 15 hours. Inset shows the comparison of cyclic voltammograms of SAM of hexadecanethiol on Au formed from ethanol (b) and the hexagonal liquid crystalline phase (c). (C) SAM of decanethiol on gold surface formed from ethanol (a) and the hexagonal liquid crystalline phase (b) by keeping the Au electrode for about 1 hour.

We have also used hexaammineruthenium(III) chloride as a redox probe molecule to evaluate the barrier property of the monolayers of decanethiol and hexadecanethiol on Au surface obtained using both the liquid crystalline phase and ethanol. Figure 4A shows the CVs obtained for bare gold and SAM of decanethiol modified Au electrodes in 1mM hexaammineruthenium(III) chloride with 0.1M lithium perchlorate as the supporting electrolyte at a potential scan rate of 50mV/s. Similarly, Figure 4B shows the comparison of cyclic voltammograms of bare Au and hexadecanethiol coated Au electrodes in the same solution. The monolayers were formed by keeping the Au sample in the corresponding thiol for about 15 hours. It can be noticed from the figure that the bare Au electrode (Figures 4A (a) and 4B (a)) shows the reversible voltammogram indicating that the ruthenium redox reaction is completely diffusion controlled. Figures 4A (b) and (c) show the cyclic voltammograms of SAM of decanethiol on Au electrodes formed from ethanol and hexagonal liquid crystalline phase respectively. It can be seen from Fig. 4A (b) that the redox reaction is quasi-reversible implying very poor blocking property of the SAM obtained using ethanol as a solvent. In contrast, the monolayer of decanethiol formed from the hexagonal liquid crystalline phase (Fig. 4A (c)) shows a complete blocking behaviour with no peak formation to ruthenium electron transfer reaction exhibiting the characteristic of an array of microelectrodes. It can also be noticed that the CVs of SAM of hexadecanethiol-modified electrodes (Fig. 4B (b) & (c)) exhibit a good blocking behaviour for the redox reaction. Even though the current values of SAM of hexadecanethiol on Au coated electrodes obtained from ethanol and hexagonal liquid crystalline phase are almost similar, a careful analysis shows the better blocking property in the latter case. This again indicates that the monolayers of decanethiol and hexadecanethiol on Au formed from the

hexagonal liquid crystalline phase are highly dense and well ordered with defect free structure when compared to the SAMs formed using ethanol as a solvent.

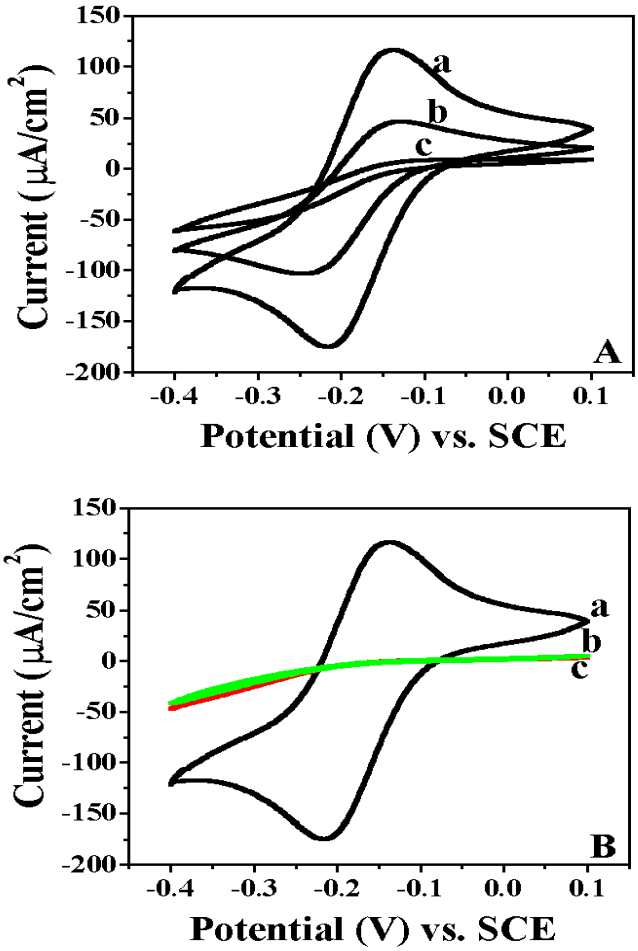

Figure 4: Cyclic voltammograms of 1mM hexaammineruthenium(III) chloride with 0.1M $LiClO_4$ as the supporting electrolyte at a potential scan rate of 50mV/s for, (A) Bare Au electrode (a), SAM of decanethiol formed from ethanol (b) and SAM of decanethiol formed from the hexagonal liquid crystalline phase (c) respectively for about 15 hours. (B) Bare Au electrode (a), SAM of hexadecanethiol on Au formed from ethanol (b) and SAM of hexadecanethiol formed from the hexagonal liquid crystalline phase (c) respectively for about 15 hours.

It is well known from literature that the adsorption of alkanethiol on Au surface in ethanol medium takes place in three steps [37]. During the first fast step the adsorption takes place in a few seconds during which time about 80% to 85% of the coverage is completed. The second and third steps extend during the rest of the time before the complete coverage is attained. The first step in the adsorption process is identified with Au-S bond formation. The second step can be linked to the straightening of the alkyl chains. The third and final step, which is the slowest relates to the reorientation of the terminal methyl end groups [37,38]. We feel that the third step of the organization of the monolayer film where the van der Waals neighbouring alkyl chain interaction takes place is significantly helped if the medium is water instead of an organic solvent. This is also supported by our earlier studies which show that adsorbing the alkanethiol monolayer for a short time of 1 hour in ethanol and subsequently keeping it in water for 6 hours forms a monolayer with better blocking properties than the SAM formed by keeping in ethanol as a medium for 24 hours [22]. This happens because the organic solvents solvate the alkyl chains and inhibits their close packing [21] while in an aqueous environment the hydrophobic interactions are maximized and tight packing of the alkyl chains is facilitated. In the case of adsorption in the hexagonal liquid crystalline phase, the organization of the alkyl chains is significantly improved by the aqueous environment and polar end groups of the cylindrical micelles neighbouring the substrate.

5.3.3.2. Electrochemical impedance spectroscopy

In order to evaluate the structural integrity of the monolayer formed from the hexagonal liquid crystalline phase in a quantitative manner, the charge transfer resistances of the SAM modified electrodes against the diffusion of the

redox probe were measured using electrochemical impedance spectroscopy. In addition the impedance data were also used to determine the surface coverage and other kinetic parameters of the monolayer coated electrodes. Figure 5B shows the impedance plots (Nyquist plots) of the monolayer of decanethiol on Au surface in equal concentrations of potassium ferro/ferri cyanide with NaF as the supporting electrolyte. Similarly, Figure 5C shows the impedance plots (Nyquist plots) of SAM of hexadecanethiol on Au electrode in the same solution. The monolayers were obtained by keeping the Au strips in the corresponding thiol solution for about 15 hours. For comparison the plot of bare Au electrode was also given in the Figure 5A. The impedance spectroscopy was carried out at a formal potential of $[Fe(CN)_6]^{3-|4-}$. It can be seen from the figure that the bare Au electrode (Fig. 5A) shows a very small semicircle at high frequency region and a straight line at low frequency region indicating that the electron transfer process of the redox couple is essentially diffusion controlled. On the other hand, the SAM modified electrodes (Figures 5B and 5C) show the formation of semicircle in the entire range of frequency used for the study implying a perfect blocking behaviour and complete charge transfer control for the electron transfer process. A very large semicircle in the cases of SAMs of decanethiol and hexadecanethiol on Au surface obtained using the hexagonal liquid crystalline phase (Figures 5B (b) and 5C (b)) when compared to the SAMs formed from ethanol (Figures 5B (a) and 5C (a)) confirms an excellent electrochemical blocking ability of SAM with the higher charge transfer resistance against the diffusion of redox probe in the former case.

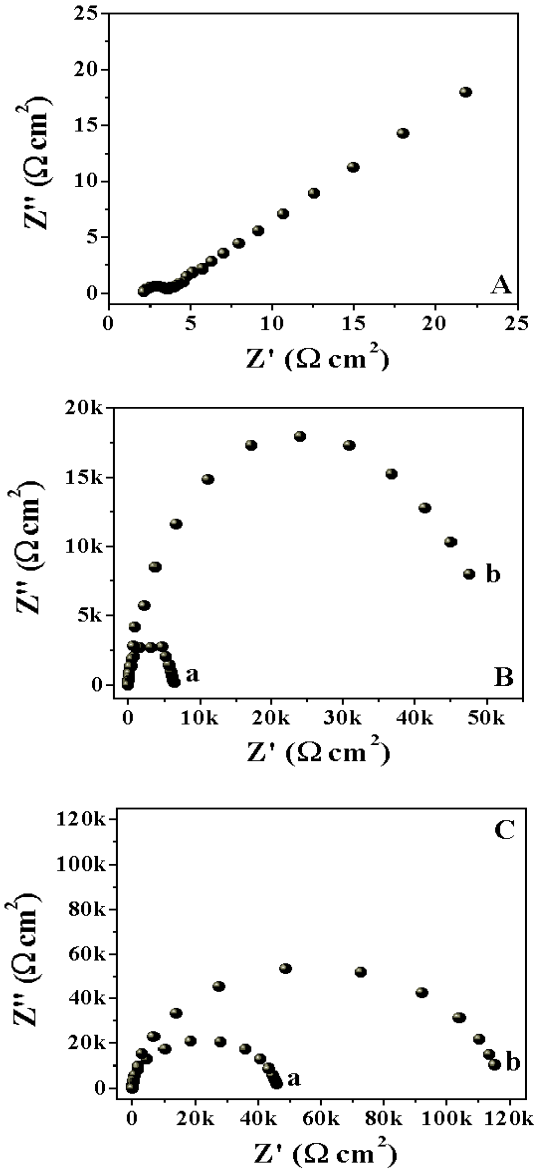

Figure 5: The impedance (Nyquist) plots in 10mM potassium ferrocyanide and 10mM potassium ferricyanide with 1M NaF as the supporting electrolyte for, (A) Bare Au electrode. (B) SAM of decanethiol on Au formed from ethanol (a) and the hexagonal liquid crystalline phase (b) respectively. (C) SAM of hexadecanethiol on Au formed from ethanol (a) and the hexagonal liquid crystalline phase (b) respectively.

Figures 6A and B show the respective Nyquist plots of bare Au electrode and decanethiol coated Au electrodes in 1mM hexaammineruthenium(III) chloride with 0.1M $LiClO_4$ as the supporting electrolyte. Similarly, Figure 6C shows the impedance plots of SAM of hexadecanethiol on Au modified electrodes in the same solution. The monolayers were formed by keeping the Au sample in the corresponding thiol for about 15 hours. It can be seen from the figure that the bare Au electrode (Fig. 6A) shows a straight line in the entire range of frequency used for the study implying a perfect diffusion controlled process for the redox couple. Figures 6B (a) and (b) show the impedance plots of SAM of decanethiol on Au formed from ethanol and hexagonal liquid crystalline phase respectively. It can be noted from Fig. 6B (a) that the SAM obtained from ethanol shows the formation of small semicircle at high frequency region and a straight line at low frequency region indicating the quasi-reversible behaviour for the redox couple, which is the result of poor blocking ability of SAM formed from ethanol. Fig. 6B (b) shows the formation of larger semicircle almost in the entire range frequency implying a good blocking ability of SAM formed from the hexagonal liquid crystalline phase towards the diffusion of redox couple. Similarly, the SAM of hexadecanethiol on Au coated electrodes (Fig. 6C) show the formation of semicircles in the entire range of frequency implying the charge transfer control for the redox couple on the monolayer modified electrodes. The formation of larger semicircle in the case of SAMs formed from the hexagonal liquid crystalline phase (Figures 6B (b) and 6C (b)) when compared to that of ethanol (Figures 6B (a) and 6C (a)) points out to the fact that a highly ordered, compact monolayer with ultra low defects have been formed in the former case. These results are in conformity with our CV results discussed earlier.

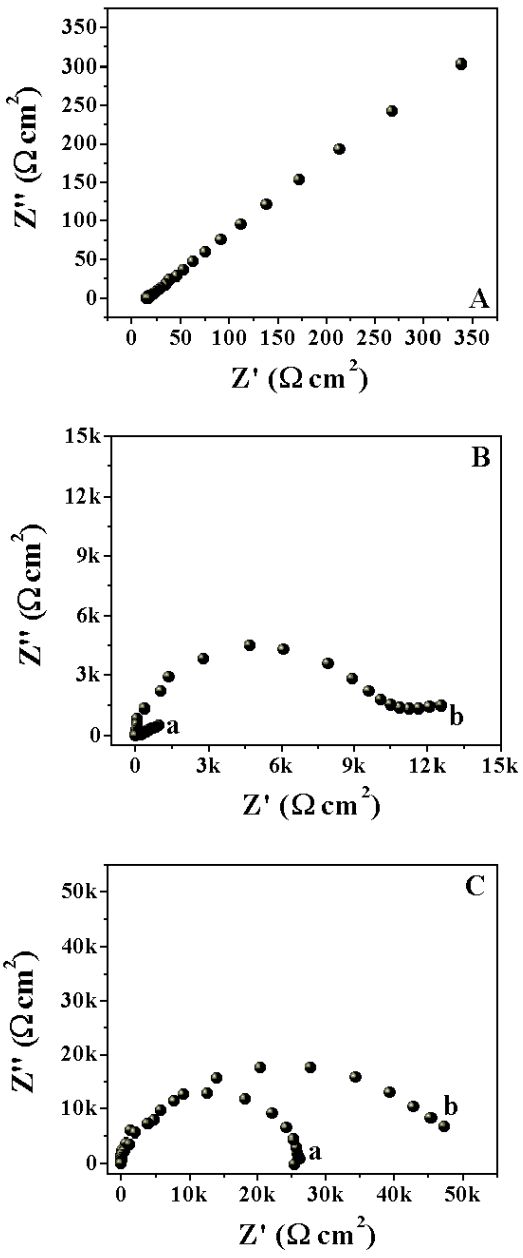

Figure 6: Typical Nyquist plots in 1mM hexaammineruthenium(III) chloride with 0.1M $LiClO_4$ as the supporting electrolyte for, (A) Bare Au electrode. (B) SAM of decanethiol on Au formed from ethanol (a) and the hexagonal liquid crystalline phase (b) respectively. (C) SAM of hexadecanethiol on Au formed from ethanol (a) and the hexagonal liquid crystalline phase (b) respectively.

5.3.3.3. Analysis of impedance data

It is well known that the diameter of semicircle obtained in the impedance plots is a measure of charge transfer resistance (R_{ct}), which is higher in the case of SAM modified electrodes when compared to that of the R_{ct} determined at bare Au electrode due to the inhibition of electron transfer rate on the monolayer coated electrodes. The impedance values are fitted to a standard Randle's equivalent circuit comprising of a parallel combination of constant phase element (CPE) represented by Q and a faradaic impedance Z_f in series with the uncompensated solution resistance, R_u. The faradaic impedance, Z_f is a series combination of charge transfer resistance, R_{ct} and the Warburg impedance, W for the cases of bare Au electrode and SAM of decanethiol on Au (for redox reaction of ruthenium complex) coated electrode. For the other cases of SAM modified electrodes, the Z_f consists only of charge transfer resistance, R_{ct}. By equivalent circuit fitting procedure using the impedance data of bare Au electrode and SAM modified electrodes, we have determined the R_{ct} values, which are shown in Table 1. It can be seen from the table that the R_{ct} values of SAM modified electrodes as expected are several orders of magnitude higher than the bare Au electrode. It can also be seen that the R_{ct} values obtained for the SAMs formed from the hexagonal liquid crystalline phase are very much higher when compared to the SAMs formed from ethanol implying the better blocking of the SAM to the redox reaction in the former case. From the R_{ct} values, we have calculated the surface coverage (θ) of the monolayer on the gold electrode using equation (1), by assuming that the current is due to the presence of pinholes and defects within the monolayer.

$$\theta = 1 - (R_{ct}/R'_{ct}) \qquad (1)$$

where R_{ct} is the charge transfer resistance of bare Au electrode and R'_{ct} is the charge transfer resistance of the corresponding SAM modified electrodes. The surface coverage values are >99.9% for almost all the SAM coated electrodes used in this work and the values are shown in Table 1.

Using the R_{ct} values obtained from the impedance plots, we have calculated the apparent rate constant values of $[Fe(CN)_6]^{3-|4-}$ and $[Ru(NH_3)_6]^{2+|3+}$ redox couples for the SAM modified electrodes. The monolayer, acting as an array of microelectrodes, provides a barrier for the electron transfer reaction leading to an expected decrease in the rate constant values. For a one electron first order reaction with $C_o=C_r=C$ and for unit geometric area, the apparent rate constant can be calculated from the following equation,

$$R_{ct} = RT/[F^2 (1-\theta) k_o C] = RT/[F^2 k_{app} C] \qquad (2)$$

where R is the gas constant, T the temperature, F the Faraday's constant, C the concentration of redox couple, (1-θ) the total fraction of pinholes, R_{ct} the charge transfer resistance, k_o and k_{app} are the real and apparent rate constants respectively. The real rate constant (k_o) for bare Au electrode and the apparent rate constants (k_{app}) for SAM modified electrodes are calculated from the corresponding charge transfer resistance (R_{ct}) values using the equation (2) and are given in Table 1. It can be seen from the table that the apparent rate constants values of SAM modified electrodes are very much lower compared to the real rate constant values of 0.1985 cm/s for $[Fe(CN)_6]^{3-|4-}$ and 2.0310 cm/s for $[Ru(NH_3)_6]^{2+|3+}$ redox couples respectively on bare Au surface. It can also be seen from the table that the apparent rate constants values of SAMs formed from the hexagonal liquid crystalline phase are an order of magnitude lower compared to the corresponding SAMs formed from ethanol in the case of decanethiol SAM implying the slower electron transfer kinetics in the former

case due to the formation highly compact, well-organized monolayer with ultra low defects. The value of k_{app} in the case of hexadecanethiol SAM formed from the liquid crystalline phase is also very much lower when compared to that of ethanol.

Table-1

The charge transfer resistance (R_{ct}), surface coverage (θ) and the rate constants (k_o & k_{app}) for bare Au electrode and SAM modified electrodes obtained from the impedance plots using $[Fe(CN)_6]^{3-|4-}$ and $[Ru(NH_3)_6]^{2+|3+}$ as redox probes.

Sample	$[Fe(CN)_6]^{3-\|4-}$			$[Ru(NH_3)_6]^{2+\|3+}$		
	R_{ct} (Ω cm^2)	θ (%)	k_o / k_{app} (cm/s)	R_{ct} (Ω cm^2)	θ (%)	k_o / k_{app} (cm/s)
Bare Au	**1.34**	--------	**0.1985**	**1.31**	--------	**2.0310**
DT in EtOH	**6.17 k**	**99.980**	**4.31×10^{-5}**	**188.65**	**99.310**	**1.41×10^{-2}**
DT in LC phase	**45.34 k**	**99.997**	**5.87×10^{-6}**	**9.95 k**	**99.987**	**2.68×10^{-4}**
HDT in EtOH	**45.04 k**	**99.997**	**5.91×10^{-6}**	**25.85 k**	**99.995**	**1.03×10^{-4}**
HDT in LC phase	**113.40 k**	**99.999**	**2.35×10^{-6}**	**44.10 k**	**99.997**	**0.60×10^{-4}**

DT → Decanethiol on Au electrode

HDT → Hexadecanethiol on Au electrode

EtOH → Ethanol as a solvent

LC → Hexagonal liquid crystalline phase

5.3.3.4. Pinhole analysis

The study of electrochemical impedance spectroscopy on the SAM modified electrodes provides valuable information on the distribution of pinholes and defects within the monolayer. Finklea et al. [39] developed a model for the impedance response of a monolayer-coated electrode, which behaves as an array of microelectrodes. Fawcett and co-workers have extensively used pinhole analysis to evaluate the structural integrity of the monolayer by determining the distribution of pinholes and defects using the electrochemical impedance data [24,25]. On the basis of the work of Matsuda [40] and Amatore [41], a model has been developed to fit the faradaic impedance data obtained for the electron transfer reactions at the SAM modified electrode to understand the distribution of pinholes and defects in the monolayer. The impedance expressions have been derived by assuming that the total pinhole area fraction, $(1-\theta)$ is less than 0.1, where θ is the surface coverage of the monolayer. Both the real and imaginary parts of the faradaic impedance values are plotted as a function of $\omega^{-1/2}$. At higher frequencies, the diffusion profiles of each individual microelectrode constituent of the array are separated, in contrast to the situation at lower frequencies where there is an overlap of diffusion profiles.

In the case of SAMs of decanethiol and hexadecanethiol on Au surface formed from ethanol and hexagonal liquid crystalline phase as the solvating medium, the presence of pinholes and defects are evaluated using the above-described model. Figures 7 (a-e) show the real part of the faradic impedance of different SAM modified electrodes as a function of $\omega^{-1/2}$. For comparison, the plot of a bare gold electrode is also shown in Fig. 7 (a). Figures 7 (b) and (c) show the plots of real components of faradaic impedance, Z'_f vs. $\omega^{-1/2}$ for the

SAM of decanethiol on Au surface formed from ethanol and hexagonal liquid crystalline phase respectively. Figures 7 (d) and (e) show the similar plots for the monolayer of hexadecanethiol on Au surface. Figures 8 (a-d) show the plots of imaginary components of faradaic impedance, Z''_f vs. $\omega^{-1/2}$ for the above-mentioned electrodes. It can be seen from the figures 7 and 8 that the faradaic impedance plots have features similar to that of an array of microelectrodes. There are two linear domains at high and low frequencies for the Z'_f vs. $\omega^{-1/2}$ plots and a peak formation corresponding to the frequency of transition between these two linear domains in the Z''_f vs. $\omega^{-1/2}$ plots. According to the model described earlier, this frequency separates the two time-dependent diffusion profiles for the microelectrodes.

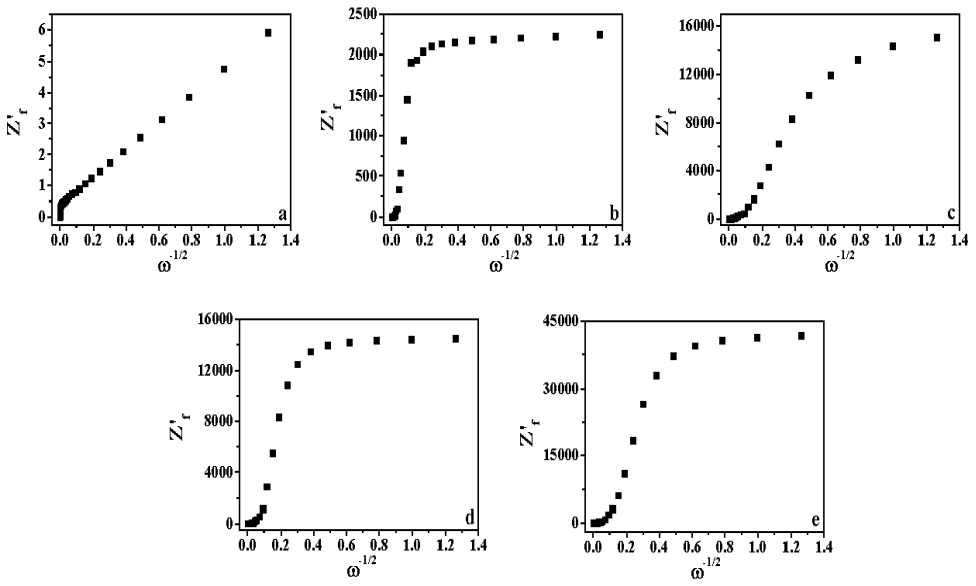

Figure 7: Plots of real parts of the faradaic impedance Z'_f vs. $\omega^{-1/2}$ for, (a) Bare Au electrode, (b) SAM of decanethiol on Au formed from ethanol, (c) SAM of decanethiol on Au formed from the hexagonal liquid crystalline phase, (d) SAM of hexadecanethiol on Au obtained using ethanol, (e) SAM of hexadecanethiol on Au obtained using the hexagonal liquid crystalline phase.

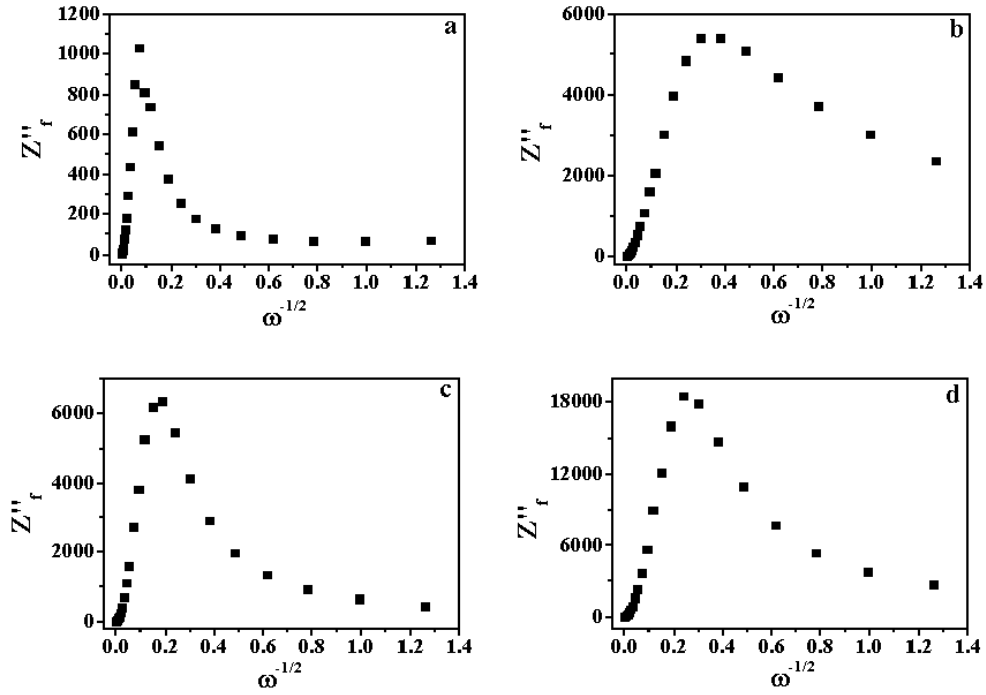

Figure 8: Plots of imaginary parts of the faradaic impedance Z''_f as a function of $\omega^{-1/2}$ for, (a) SAM of decanethiol on Au obtained using ethanol, (b) SAM of decanethiol on Au obtained using the hexagonal liquid crystalline phase, (c) SAM of hexadecanethiol on Au formed from ethanol, (d) SAM of hexadecanethiol on Au formed from the hexagonal liquid crystalline phase.

The surface coverage (θ) of the monolayer can be determined from the slope of the Z'_f vs. $\omega^{-1/2}$ plot at a higher frequency region and is given by [24,25],

$$m = \sigma + \sigma / (1- \theta) \quad (3)$$

and $$\theta = 1- [\sigma / (m-\sigma)] \quad (4)$$

where m is the slope obtained from the faradaic impedance plots, θ the surface coverage of the monolayer and σ the Warburg coefficient, which can be obtained from the unmodified bare gold electrode.

It can be seen from Fig. 7 that at lower frequency the slope of the curve is decreasing as a function of $\omega^{-1/2}$. We also find the Warburg coefficient (slope m) calculated for the SAM modified electrodes is always greater than that obtained from the bare gold electrode (σ). The increase in the apparent value of the Warburg coefficient for monolayer-coated electrodes suggests that the pinholes are distributed in patches over the surface. From the analysis of Fig. 7 and using the equations (3) and (4), we have calculated the surface coverage values of 0.99980 and 0.99992 for the monolayer of decanethiol and 0.99993 and 0.99997 for the monolayer of hexadecanethiol obtained using ethanol and hexagonal liquid crystalline phase as the solvating medium respectively. These values are in good agreement with the surface coverage values determined from the R_{ct} values.

5.3.3.5. Study of ionic permeability of SAM

The insulating properties of SAM have been evaluated by studying the ionic permeation in an inert electrolyte without any redox species using electrochemical impedance spectroscopy. Boubour and Lennox have extensively studied the insulating properties of self-assembled monolayers of n-alkanethiols and ω-functionalized n-alkanethiols using impedance spectroscopy in an inert electrolyte of K_2HPO_4 [42-44]. From the measurement of phase angle at an ion-diffusion-related frequency (1Hz), these authors have classified the SAMs to a pure capacitor ($\geq 88^0$) and a leaky capacitor ($<87^0$) contaminated by a resistive component associated with the current leakage at defect sites.

Fawcett et al. [24,25] have studied the ionic permeability of the monolayers of alkanethiol in $NaClO_4$ and tetrapropylammonium perchlorate (TPAP) using impedance spectroscopy and correlated to the structural defects and pinholes in the SAM. In this work, we have used NaF as an inert electrolyte to evaluate the ionic permeability of the SAM modified electrodes. The ionic sizes of Na^+ and F^- ions are smaller compared to previously reported electrolytes. We have used NaF in order to probe the insulating properties of SAM to ionic permeability for very small ions such as Na^+ and F^- ions. We have used impedance spectroscopy as a tool for evaluation at a wider frequency ranging from 100kHz to 0.1Hz.

Figures 9A and 9B show the respective Bode phase angle plots of SAMs of decanethiol and hexadecanethiol on Au formed from ethanol (a) and hexagonal liquid crystalline phase (b) in 1M NaF solution without any redox species. The monolayers were formed by keeping the Au strips in the corresponding thiol solution for about 15 hours. It can be seen from the figures that the phase angle values of the SAMs formed from the hexagonal liquid crystalline phase (Figures 9A (b) and 9B (b)) are higher when compared to the SAMs formed from ethanol (Figures 9A (a) and 9B (a)). This implies that the ionic permeation is lower and the SAM possesses better insulating properties when the hexagonal liquid crystalline phase is used as a solvating medium. This conclusion has been further strengthened by the fact that the impedance values are higher and the SAM shows an ideal capacitive behaviour in the former case, as can be seen form the figure 10. We have obtained a phase angle of 86^0 and 84^0 at 1Hz and 82^0 and 63^0 at 0.1Hz for the SAM of decanethiol on Au obtained from the hexagonal liquid crystalline phase and ethanol respectively. Similarly, we have obtained a phase angle of 88^0 and 86^0 at 1Hz and 86^0 and 82^0 at 0.1Hz for the SAM of hexadecanethiol on Au formed from the hexagonal liquid crystalline phase and ethanol respectively.

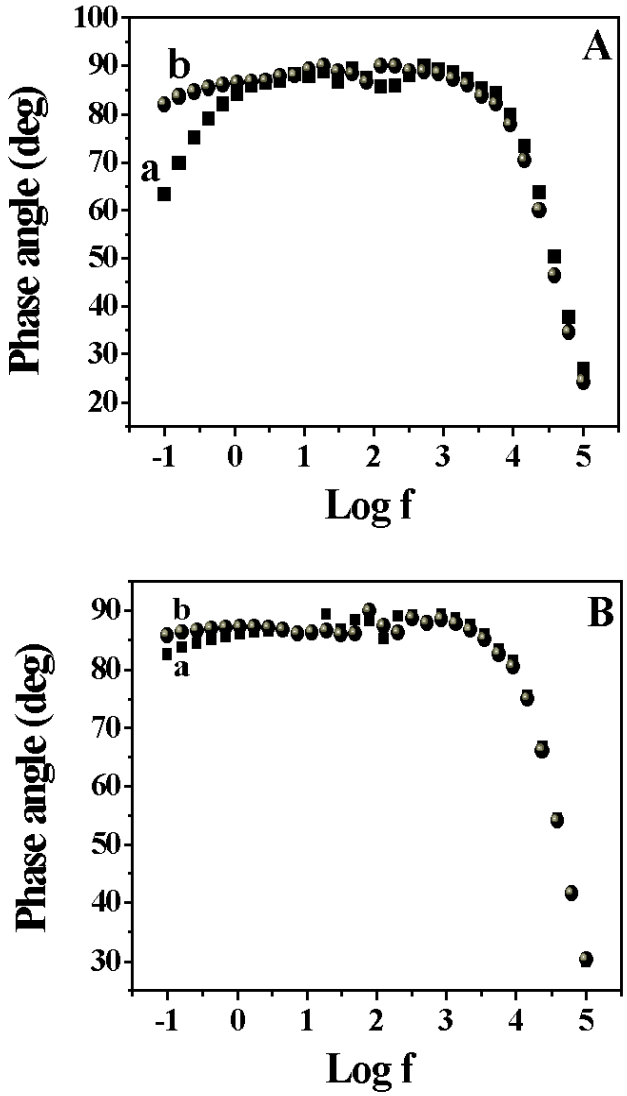

Figure 9: Bode phase angle plots in 1M NaF aqueous solution for, (A) SAM of decanethiol on Au (15 hours) formed from ethanol (a) and from the hexagonal liquid crystalline phase (b) respectively. (B) SAM of hexadecanethiol on Au (15 hours) prepared from ethanol (a) and from the hexagonal liquid crystalline phase (b) respectively.

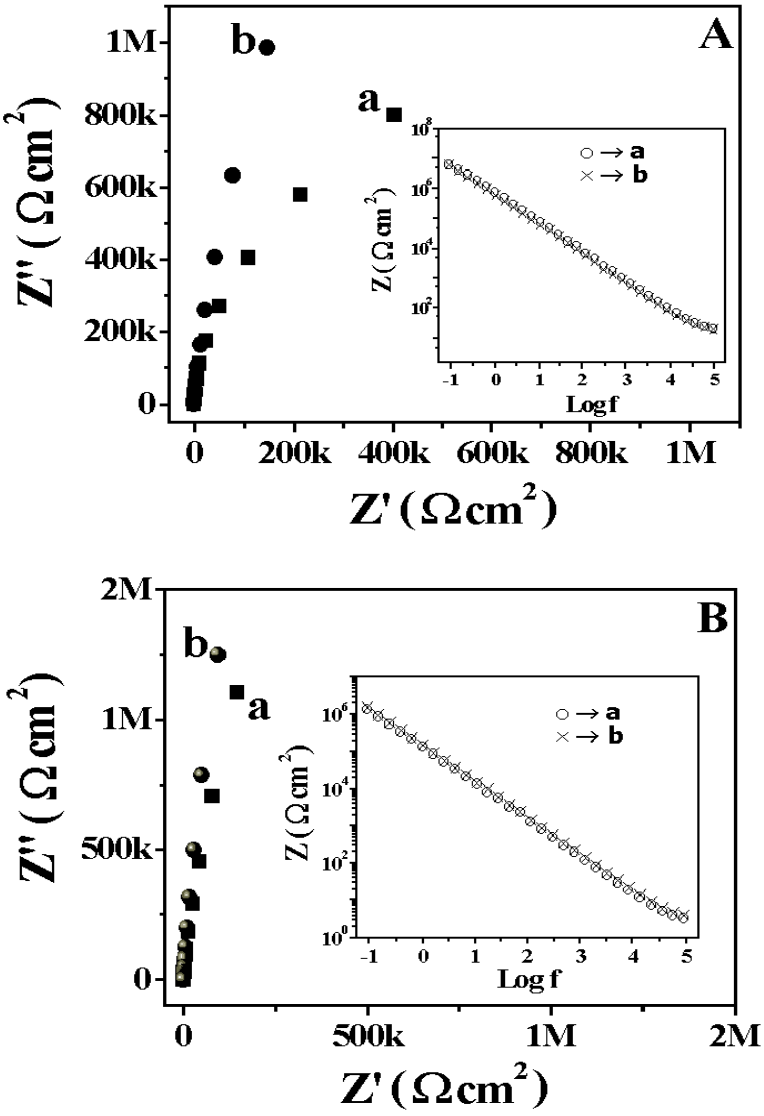

Figure 10: Nyquist plots in 1M NaF aqueous solution for, (A) SAM of decanethiol on Au (15 hours) formed from ethanol (a) and from the hexagonal liquid crystalline phase (b) respectively. Inset shows the total impedance (Z) vs. frequency (in logarithmic scale) for the same electrodes. (B) SAM of hexadecanethiol on Au (15 hours) prepared from ethanol (a) and from the hexagonal liquid crystalline phase (b) respectively. Inset shows the total impedance (Z) vs. frequency (in logarithmic scale) for the same electrodes.

Figure 10 shows the Nyquist plots in 1M NaF aqueous solution for the SAMs of decanethiol (A) and hexadecanethiol (B) on Au (about 15 hours) surface formed from ethanol (a) and the hexagonal liquid crystalline phase (b) respectively. The insets show the plots of total impedance vs. frequency for the same electrodes. It can be seen from the figures that the impedance values are higher and the monolayers show an ideal capacitive behaviour when the hexagonal liquid crystalline phase is used as an adsorbing medium. This implies that the SAMs obtained using the hexagonal liquid crystalline phase can be viewed as a pure capacitor with almost defect free structure and the SAMs formed from ethanol act as a leaky capacitor with the current path provided through the pinholes and defects in the monolayer. The higher phase angle obtained in the case of SAMs prepared from the hexagonal liquid crystalline phase even at lower frequencies, where ionic permeation is generally favoured, points out to the fact that a compact, dense monolayer has been formed with very low defects.

5.3.3.6. Determination of capacitance of the monolayer

The capacitance values of the monolayer-coated electrodes have been determined by carrying out the electrochemical impedance spectroscopy studies in a solution containing pure supporting electrolyte without any redox species. In the present study, we have used 1M NaF as an inert electrolyte. The impedance measurements were carried out at a potential of 0.0V vs. SCE using a wider frequency ranging from 100 mHz to 100 kHz. The capacitance values were measured from the imaginary component of impedance at the high frequency pseudoplateau region [38] of the capacitance vs. frequency (in log scale) plots (Figures not shown). We have determined the capacitance values of 1.21 $\mu F/cm^2$ and 1.02 $\mu F/cm^2$ for the respective SAMs of decanethiol and

hexadecanethiol on Au surface obtained using the lyotropic hexagonal liquid crystalline phase as a solvating medium and these values are slightly higher for the corresponding monolayers formed from ethanol. The measured capacitance values are in good agreement with the values reported by Boubour and Lennox [43,44] and Bilewicz et al. [45] for the monolayers of decanethiol and hexadecanethiol on Au surface. These observations rule out the possibilities of any multilayer formation or the adsorption of surfactant (Triton X-100 in this case) molecules on the monolayer.

5.3.3.7. Grazing angle FTIR spectroscopy

We have carried out grazing angle FTIR spectroscopy on the SAM modified surfaces to characterize its orientation and packing when the hexagonal lyotropic liquid crystalline phase is used as a solvating medium. Figure 11 shows the FTIR spectra in the CH stretching region for the SAM of decanethiol (A) and hexadecanethiol (B) on Au surface formed from the hexagonal liquid crystalline phase. The peaks at 2851 cm^{-1} and 2920 cm^{-1} are assigned to the symmetric (ν_s (CH_2)) and asymmetric ((ν_a (CH_2)) stretching due to methylene (-CH_2) group. Further the peaks at 2878 cm^{-1}, 2936 cm^{-1} and 2963 cm^{-1} are assigned to symmetric stretching due to Fermi Resonance (FR) splitting (ν_s (CH_3, FR)) and asymmetric stretching (ν_a (CH_3)) due to methyl (-CH_3) group. The peak positions of both ν_a (CH_2)) and ν_s (CH_2)) are indicative of crystalline-like packing of the alkyl chains, which implies the presence of all-trans conformational sequences in the alkyl chains [46]. The peaks positions of decanethiol and hexadecanethiol formed from both the hexagonal liquid crystalline phase and ethanol as a solvating medium are almost the same and for

simplicity we have provided here only the FTIR spectra formed from the liquid crystalline phase.

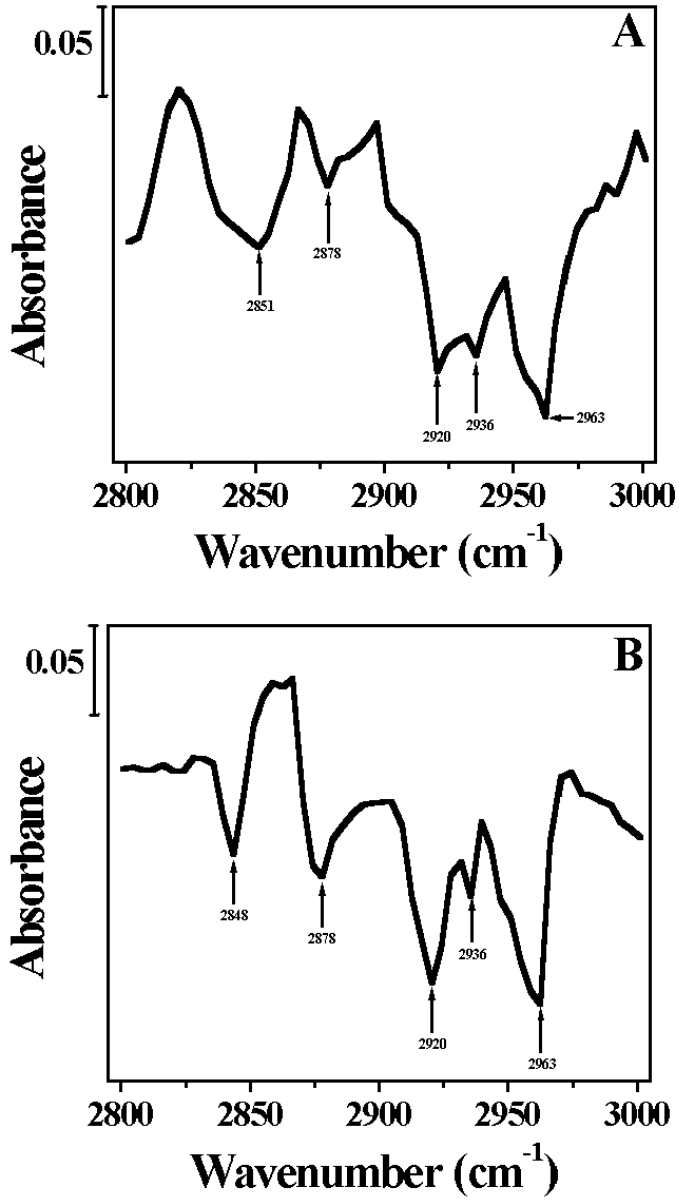

Figure 11: Grazing angle FTIR spectra of (A) decanethiol and (B) hexadecanethiol monolayers on Au surface formed from the hexagonal liquid crystalline phase by keeping the Au strips for about 15 hours in the corresponding thiol solution.

The peak positions agree with the reported values for the monolayers of decanethiol and hexadecanethiol on Au surface [47-50]. However, we do not see any peaks due to the aromatic ring C-C stretching and C-H stretching modes in the spectra indicating the absence of phenyl ring (from the surfactant) on the SAM modified surface. This rules out the possibility of adsorption of Triton X-100 (surfactant) or any other impurities on the monolayer-coated electrodes.

Jennings et al. [30-33] have proposed a mechanism for the formation of alkanethiolate SAMs from the aqueous micellar solution. We feel that a similar process may be operating in the case of hexagonal liquid crystalline phase also. However, this needs further experimental support. It is clear that the use of aqueous medium eliminates the problem associated with the intercalation of solvent molecules thereby providing the way for better inter chain interactions among alkanethiols. The formation of homogeneous mixture of the hexagonal liquid crystalline phase after the addition of thiol implies a complete solubilization of thiol in the hexagonal liquid crystalline phase. Based on these observations, we have proposed a plausible mechanism for the monolayer formation in the hexagonal liquid crystalline phase and it has been explained briefly in the later section.

II. SAMs OF AROMATIC THIOLS ON GOLD SURFACE

5.4. Introduction

As with aliphatic thiols, we have also studied and evaluated the barrier properties of monolayers of some aromatic thiols on gold surface using the hexagonal liquid crystalline phase as an adsorbing medium. We have formed the monolayers of thiophenol (TP), p-aminothiophenol (p-ATP) and 2-naphthalenethiol (NT) on gold surface and they have been characterized using electrochemical techniques. As mentioned earlier, the hexagonal liquid crystalline phase consists of water and Triton X-100 components at a particular composition. The hexagonal structure of the liquid crystalline phase is confirmed by polarizing light microscopic textural studies and it is found that even after the addition of aromatic thiol the hexagonal structure of the liquid crystalline phase is maintained. In contrast to well-studied SAMs of aliphatic thiols, there is also a great deal of interest on the monolayers of aromatic thiols [51-54] in recent times. SAMs of aromatic thiols are of interest owing to their higher rigidity and the presence of delocalized π-electrons in the aromatic ring. It is essential to study and investigate the electron transfer reactions on these aromatic SAM modified surfaces in order to understand the potential applications of these SAMs in many devices and technologically important processes in molecular electronics where the monolayer acts as a molecular wire for electron transport. In the previous chapter we have discussed the monolayer formation of these above-mentioned aromatic thiols on gold surface using ethanol as a solvent. We have tried to improve the blocking property of these SAMs by potential cycling, annealing and using mixed SAM formation and the results were discussed elaborately in the previous chapter. Here we have used the hexagonal liquid crystalline phase as an adsorbing medium for the monolayer formation and evaluated their barrier property using two different

redox couples viz., $[Fe(CN)_6]^{3-|4-}$ and $[Ru(NH_3)_6]^{2+|3+}$ as probe molecules. Electrochemical techniques such as cyclic voltammetry (CV) and electrochemical impedance spectroscopy (EIS) were extensively used for the electron transfer studies. Impedance spectroscopy data were used for the calculation of surface coverage and other kinetic parameters for the SAM modified electrodes. We have also compared our results with that of the corresponding aromatic SAMs on gold surface obtained using ethanol as a solvent.

5.5. Experimental section

5.5.1. Chemicals

Thiophenol (Aldrich), p-aminothiophenol (Aldrich), 2-naphthalenethiol (Aldrich), ethanol 99.95% (Merck), Triton X-100 (Spectrochem), potassium ferrocyanide (Loba), potassium ferricyanide (Qualigens), hexaammineruthenium(III) chloride (Alfa Aesar), sodium fluoride (Qualigens) and lithium perchlorate (Acros Organics) were used in this study as received. All the chemical reagents used in this work were analytical grade (AR) reagents. Millipore water having a resistivity of 18 MΩ cm was used to prepare the aqueous solutions. The structures of the aromatic thiols used for the monolayer study is shown below.

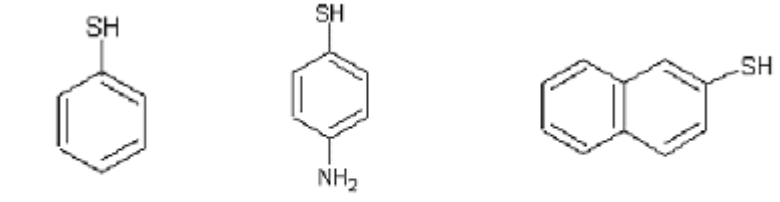

Thiophenol **p-Aminothiophenol** **2-Naphthalenethiol**

5.5.2. Preparation of the hexagonal liquid crystalline phase

The lyotropic liquid crystalline phase is a mixture of Triton X-100 (42% by weight) and water (58% by weight) [34], which exhibits the broken mosaic and focal conic textures of the hexagonal phase in textural studies using polarizing light microscopy. The hexagonal structure of the liquid crystalline phase is also confirmed by X-ray diffraction studies, as described earlier. For the preparation of aromatic SAMs, the aromatic thiols were added to the above-mentioned liquid crystalline phase. About 5mg of the compound (in the case of NT and p-ATP) and 2ml of neat thiol (in the case of TP) were added to the total volume of 25ml of the hexagonal liquid crystalline phase. Initially, the hexagonal liquid crystalline phase was heated to the isotropic phase at around 40^0C – 45^0C into which the thiol was added and stirred completely to obtain a homogeneous mixture of solution. Then it was allowed to cool down to room temperature and used for the SAM preparation. Even after the addition of thiol, the hexagonal structure of the liquid crystalline phase is maintained and it was confirmed by polarizing light microscopy.

5.5.3. Sample preparation

Gold sample of purity 99.99% was obtained from Arora Mathey, India. Evaporated gold (~100 nm thickness) on glass with chromium underlayers (~ 2-5 nm thickness) was used for the monolayer formation and its characterization using electrochemical techniques. The substrate was heated to 350^0C during gold evaporation under a vacuum pressure of 2 X 10^{-5} mbar, a process that normally yields a very smooth gold substrate with predominantly Au (111) orientation. The evaporated gold samples were used as strips for SAM formation and its analysis.

For electrochemical characterization, a conventional three-electrode electrochemical cell was used. A platinum foil of large surface area was used as a counter electrode and a saturated calomel electrode (SCE) was used as a reference electrode with the aromatic SAM modified gold electrode as a working electrode. The cell was thoroughly cleaned before each experiment and kept in a hot air oven at 100^0C for at least 1 hour before the start of the experiment.

5.5.4. Preparation of aromatic SAMs using the hexagonal liquid crystalline phase

Before SAM formation, the evaporated Au strips were pre-treated with "piranha" solution (It is a mixture of 30% H_2O_2 and Conc. H_2SO_4 in 1:3 ratio) and washed completely with millipore water. The monolayers of aromatic thiols such as TP, p-ATP and NT were prepared by keeping the Au strips in the hexagonal liquid crystalline phase containing the corresponding thiol for about 15 hours at room temperature. After this, the electrode was thoroughly washed with a jet of distilled water and finally with millipore water. For comparison, we have also prepared the monolayers of these aromatic thiols on Au surface using ethanol as a solvent. In this case, the evaporated Au strips were dipped in 1mM thiol in ethanol solution for about 15 hours at room temperature. Upon removal, the SAM coated electrodes were rinsed with ethanol, washed with distilled water and finally with millipore water and immediately used for the analysis.

5.5.5. Electrochemical characterization of aromatic SAMs on Au surface

Cyclic voltammetry and electrochemical impedance spectroscopy were used for the characterization of aromatic SAMs on gold surface and evaluation

of their barrier property by studying the electron transfer reactions on the SAM modified surfaces using two different redox probes namely potassium ferrocyanide (negative redox probe) and hexaammineruthenium(III) chloride (positive redox probe). Cyclic voltammetry was performed in solutions of 10mM potassium ferrocyanide containing 1M sodium fluoride as a supporting electrolyte at a potential range of –0.1V to 0.5V vs. SCE and 1mM hexaammineruthenium(III) chloride having 0.1M lithium perchlorate as the supporting electrolyte at a potential range of –0.4V to 0.1V vs. SCE. The impedance measurements were carried out using an ac signal of 10mV amplitude at a formal potential of the redox couple using a wide frequency range of 100kHz to 0.1Hz, in solution containing always equal concentrations of both the oxidized and reduced forms of the redox couple namely, 10mM potassium ferrocyanide and 10mM potassium ferricyanide in 1M NaF. All the experiments were performed at room temperature.

5.5.6. Instrumentation

Cyclic voltammetry was carried out using an EG&G potentiostat (model 263A) interfaced to a computer through a GPIB card (National Instruments). The potential ranges and scan rates used are shown in the respective diagrams. For electrochemical impedance spectroscopic studies the potentiostat was used along with an EG&G 5210 lock-in-amplifier controlled by Power Sine software. The electrochemical impedance spectroscopy data were used for the equivalent circuit fitting analysis using Zsimpwin software (EG&G) developed on the basis of Boukamp's model. Based on this procedure, the charge transfer resistance values (R_{ct}) of the SAM modified electrodes were calculated, from which the surface coverage (θ) values of these monolayers on Au surface were also determined.

5.6. Results and discussion

5.6.1. Electrochemical characterization

5.6.1.1. Cyclic voltammetry

Cyclic voltammetry is an excellent technique to assess the quality of the monolayer and its barrier property by studying the electron transfer reaction of redox probe molecule on the SAM modified surfaces. The aromatic SAMs of thiophenol (TP), p-aminothiophenol (p-ATP) and 2-naphthalenethiol (NT) on gold surface were formed from the hexagonal liquid crystalline phase containing the respective thiol. For comparison the corresponding monolayers obtained using ethanol as a solvent were also characterized. Figure 12 shows the cyclic voltammograms of bare Au electrode and aromatic SAMs coated Au electrodes in 10mM potassium ferrocyanide with 1M NaF as the supporting electrolyte at a potential scan rate of 50mV/s. Figures 12B, C and D show the respective cyclic voltammograms of SAMs of TP, p-ATP and NT on Au surface in the same solution. For comparison, the cyclic voltammogram of bare Au electrode is shown in figure 12A. We have compared the monolayers of these aromatic thiols formed from both the hexagonal liquid crystalline phase (a) and ethanol (b) as adsorbing media. These monolayers were formed by keeping the Au strips in the corresponding thiol solution for about 15 hours. It can be seen from the figure that the bare Au electrode (Fig. 12A) shows a perfect reversible voltammogram for the redox couple indicating that the electron transfer reaction is completely diffusion controlled. In contrast, the monolayers of aromatic thiols in the cases of thiophenol (Fig. 12B) and 2-naphthalenethiol (Fig. 12D) do not show any peak formation as the redox reaction is completely blocked by the monolayer. On the other hand, the monolayer of p-ATP on Au surface (Fig. 12C) shows a peak shaped voltammogram indicating that the electron transfer reaction is diffusion

controlled and the monolayer has a very poor blocking property. It can be observed from the figure 12C that the peak current values for the reverse peak is smaller when compared to that of the forward peak due to the change in concentration at the interface and the excessive concentration of Fe^{2+} ions at the interface arising from the aqueous solution used for the cyclic voltammetric studies.

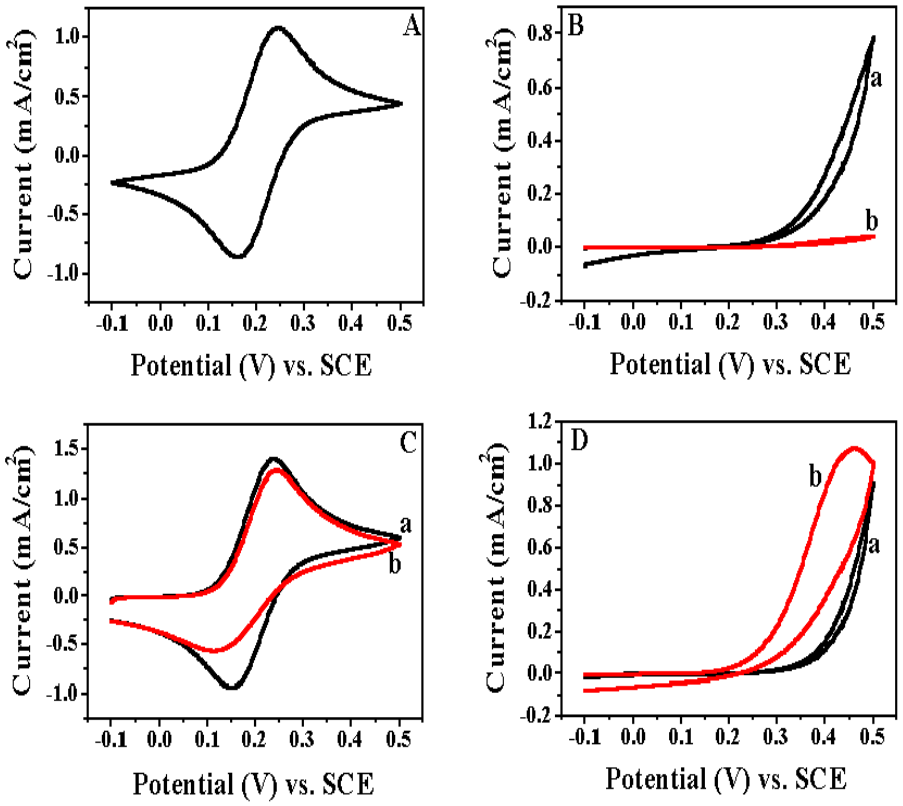

Figure 12: Cyclic voltammograms in 10mM potassium ferrocyanide with 1M NaF as a supporting electrolyte at a potential scan rate of 50 mV/s for (A) Bare Au electrode, (B) SAM of TP on Au, (C) SAM of p-ATP on Au and (D) SAM of NT on Au surface respectively. Here (a) represents the monolayer obtained using the hexagonal liquid crystalline phase and (b) denotes the monolayer formed from ethanol as a solvent.

It can be seen from the figures that the monolayers formed from the hexagonal liquid crystalline phase (a) do not show any improvement in their blocking behaviour when compared to the one obtained using ethanol (b) as a solvent. In the case of thiophenol (Fig. 12B), the SAM obtained using ethanol (b) shows the better blocking property when compared to the one formed from the hexagonal liquid crystalline phase (a) and in the case of 2-naphthalenethiol on Au (Fig. 12D) there is not much difference between the two although the current value is lower for the SAM obtained using the hexagonal liquid crystalline phase (a). These monolayers exhibit current-voltage characteristics similar to that of a microelectrode array, indicating the presence of pinholes and defects in these monolayers on gold surface. The small current flow arises due to the access of the redox species to the gold surface through these pinholes and defects present in the SAM. On the other hand, the SAM of p-ATP on Au surface (Fig. 12C) shows the quasi-reversible voltammogram indicating the diffusion-controlled process for the electron transfer reaction. In this case, the monolayers obtained using both the hexagonal liquid crystalline phase (a) and ethanol (b) as adsorbing media, do not show any blocking behaviour to the redox reaction implying the formation of a very poor SAM of p-ATP on Au surface.

We have also used hexaammineruthenium(III) chloride as a redox probe molecule to evaluate the barrier property of these monolayers of aromatic thiols on Au surface obtained using both the liquid crystalline phase and ethanol as adsorbing media. Figure 13 shows the cyclic voltammograms obtained for bare gold and the aromatic SAMs coated Au electrodes in 1mM hexaammineruthenium(III) chloride with 0.1M lithium perchlorate as the supporting electrolyte at a potential scan rate of 50mV/s.

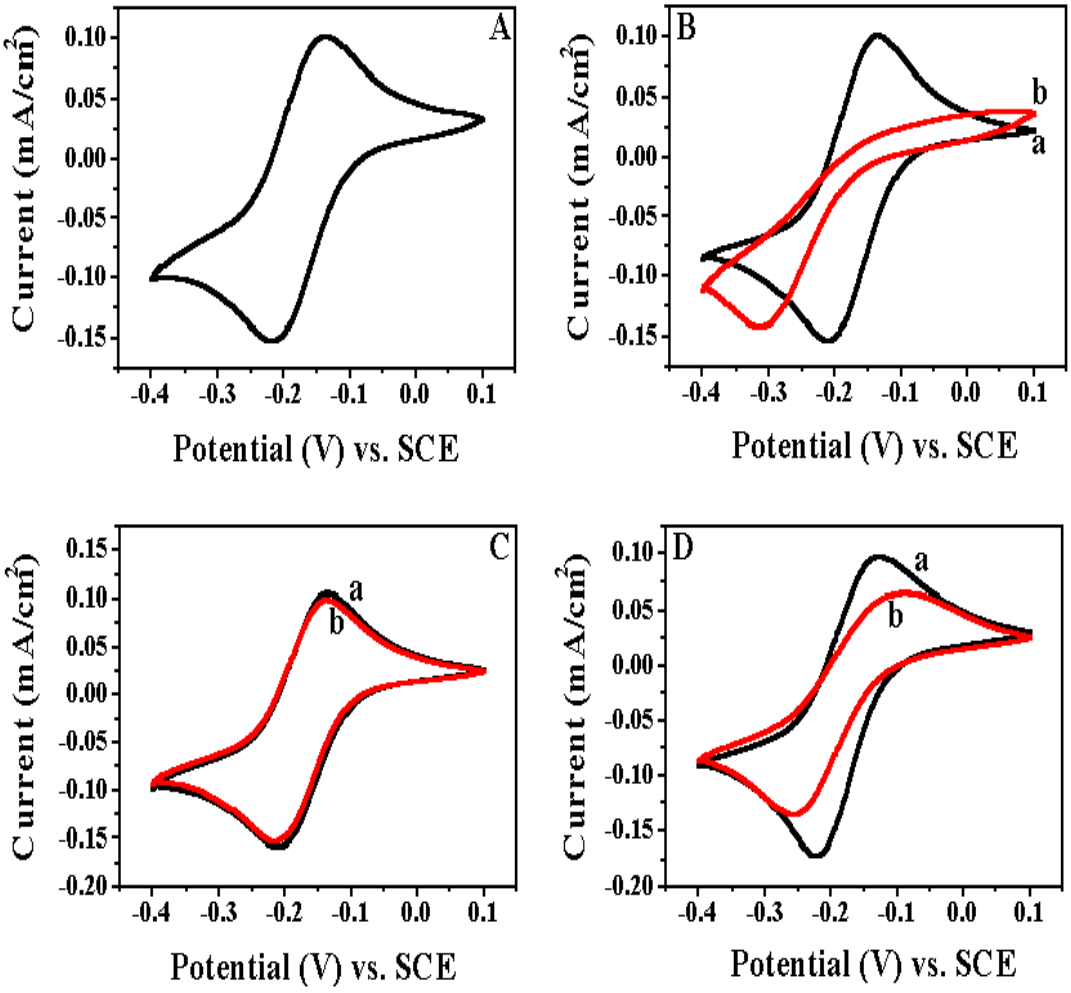

Figure 13: Cyclic voltammograms in 1mM hexaammineruthenium(III) chloride with 0.1M $LiClO_4$ as a supporting electrolyte at a potential scan rate of 50 mV/s for (A) Bare Au electrode, (B) SAM of TP on Au, (C) SAM of p-ATP on Au and (D) SAM of NT on Au surface respectively. Here (a) represents the monolayer obtained using the hexagonal liquid crystalline phase and (b) denotes the monolayer formed from ethanol as a solvent.

Figures 13B, C and D show the respective cyclic voltammograms of SAMs of TP, p-ATP and NT on Au surface in the same solution. For comparison, the CV of bare Au electrode is also shown in the figure 13A. We have compared the blocking ability of the monolayers obtained using both the hexagonal liquid crystalline phase (a) and ethanol (b). These monolayers were prepared by keeping the Au sample in the corresponding aromatic thiol for about 15 hours. It can be noticed from the figure that the bare Au electrode (Fig. 13A) shows the reversible voltammogram indicating that the ruthenium redox reaction is completely diffusion controlled. It can be seen from the figure 13B that the SAM of TP formed from the hexagonal liquid crystalline phase (a) shows a peak shaped voltammogram indicating that the ruthenium redox reaction is diffusion controlled in contrast to the monolayer obtained using ethanol (b) as a solvent, which shows a blocking behaviour. Similarly, the SAM of NT on Au (Fig. 13D) shows a complete diffusion controlled process for the redox reaction when the monolayer is formed from the hexagonal liquid crystalline phase (a) and exhibits a quasi-reversible behaviour when it is prepared using ethanol (b) as a solvent. On the other hand, the monolayer of p-ATP on Au (Fig. 13C) shows a perfect reversible voltammogram in both the cases of adsorptions implying a very poor blocking ability of the monolayer. The mechanism of electron transfer process in the case of ruthenium redox couple is discussed in detail in the previous chapter. We believe that a similar mechanism of bridge mediated electron transfer through aromatic π-electrons occur in this case also. From these results, it is clear that the monolayers of aromatic thiols formed using the hexagonal liquid crystalline phase as an adsorbing medium, do not show any improvement in their blocking ability towards the redox reactions.

5.6.1.2. Electrochemical impedance spectroscopy

In order to evaluate the structural integrity of the monolayer formed from the hexagonal liquid crystalline phase in a quantitative manner, the charge transfer resistance (R_{ct}) values of the SAM modified electrodes against the diffusion of the redox probe were measured using electrochemical impedance spectroscopy. In addition the impedance data were also used to determine the surface coverage and other kinetic parameters of the monolayer coated electrodes. Figure 14 shows the impedance plots (Nyquist plots) of the monolayers of aromatic thiols on Au surface in equal concentrations of potassium ferro/ferri cyanide with NaF as the supporting electrolyte. For comparison the impedance plot of bare Au electrode in the same solution was also given in the figure 14A. These monolayers of aromatic thiols were obtained by keeping the Au strips in the corresponding thiol solution for about 15 hours. The impedance spectroscopy was carried out at a formal potential of $[Fe(CN)_6]^{3-|4-}$ redox couple. In all these figures (a) represents the monolayer formed from the hexagonal liquid crystalline phase and (b) denotes the monolayer obtained using ethanol as a solvent. It can be seen from the figure that the bare Au electrode (Fig. 14A) shows a very small semicircle at high frequency region and a straight line at low frequency region indicating that the electron transfer process of the redox couple is essentially diffusion controlled. On the other hand, the SAM modified electrodes in the cases of TP and NT (Figures 14B and 14D) show the formation of semicircle in the entire range of frequency used for the study implying a perfect blocking behaviour and complete charge transfer control for the electron transfer process. In contrast, the SAM of p-ATP on Au (Fig. 14C) shows a semicircle at high frequency region and a straight line at low frequency region indicating a quasi-reversible

behaviour for the redox reaction, which implies a poor blocking ability of the monolayer.

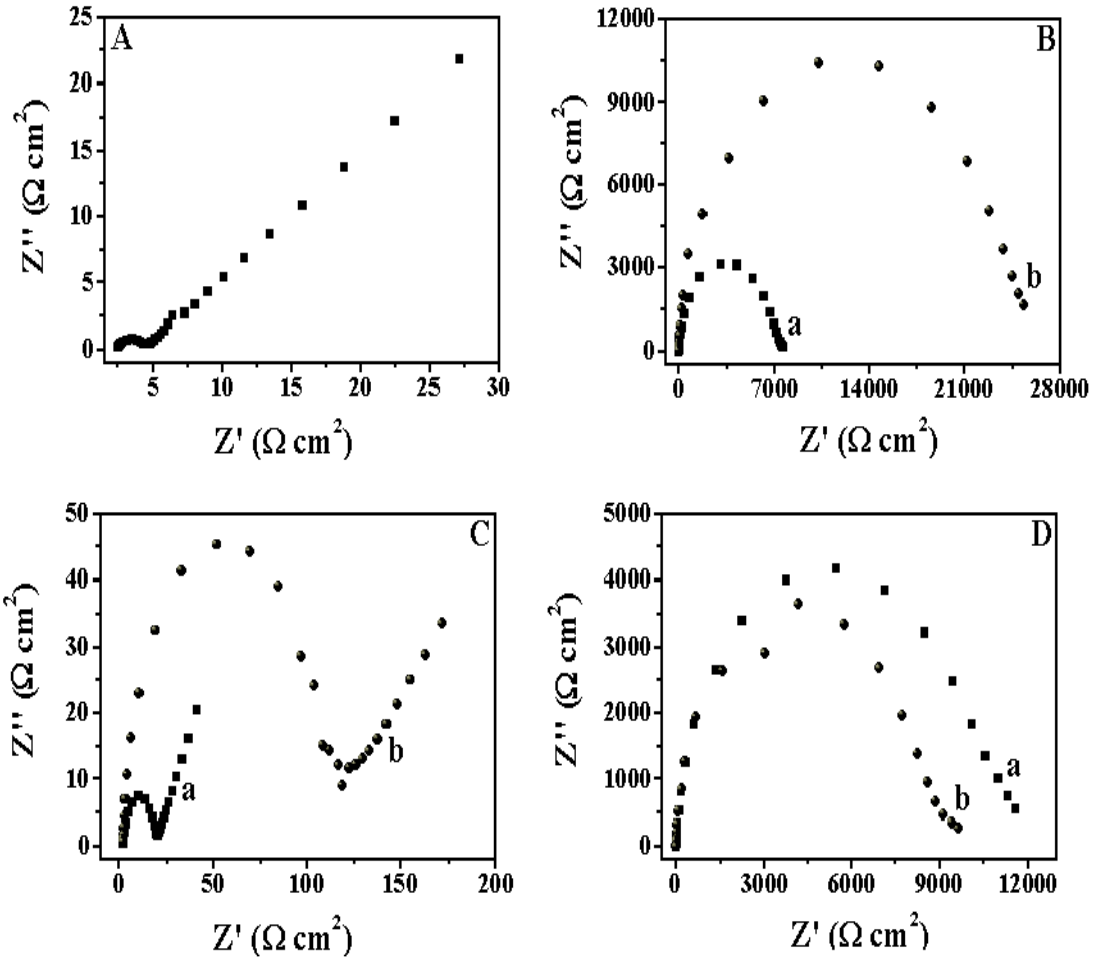

Figure 14: Impedance (Nyquist) plots in 10mM potassium ferrocyanide and 10mM potassium ferricyanide with 1M sodium fluoride as a supporting electrolyte for, (A) Bare Au electrode, (B) SAM of TP on Au, (C) SAM of p-ATP on Au and (D) SAM of NT on Au surface respectively. Here (a) represents the monolayer formed from the hexagonal liquid crystalline phase and (b) denotes the monolayer obtained using ethanol as a solvent.

It is well known in the literature that the diameter of the semicircle obtained in the impedance plot is a measure of the charge transfer resistance (R_{ct}), which denotes the extent of blocking ability of the monolayer towards the redox reaction. A very large semicircle obtained in the cases of SAMs of TP and p-ATP on Au surface obtained using ethanol (Figures 14B (b) and 14C (b)) as a solvent when compared to the corresponding SAMs formed from the hexagonal liquid crystalline phase (Figures 14B (a) and 14C (a)) confirms an excellent electrochemical blocking ability of the SAM with the higher charge transfer resistance against the diffusion of redox probe in the former case. In the case of SAM of NT on Au (Fig. 14 D), the R_{ct} value is slightly higher when it is prepared from the hexagonal liquid crystalline phase (a) when compared to the corresponding R_{ct} value obtained using ethanol (b) as a solvent. This indicates the formation of ordered, compact and dense monolayer with low defect density in the former case.

Similarly, we have used hexaammineruthenium(III) chloride as a redox probe to evaluate the blocking property of these monolayers of aromatic thiols on gold surface. Figure 15 shows the Nyquist plots of bare Au electrode and SAMs of aromatic thiols coated Au electrodes in 1mM hexaammineruthenium(III) chloride with 0.1M $LiClO_4$ as the supporting electrolyte. Figures 15B, C and D show the respective impedance plots of SAMs of TP, p-ATP and NT on Au surface. For comparison the impedance plot of bare gold electrode in the same solution is also shown in figure 15A. The monolayers of these aromatic thiols were formed by keeping the Au sample in the corresponding thiol for about 15 hours. In all these figures, (a) represents the monolayer obtained using the hexagonal liquid crystalline phase and (b) denotes the corresponding monolayer formed from ethanol as a solvent.

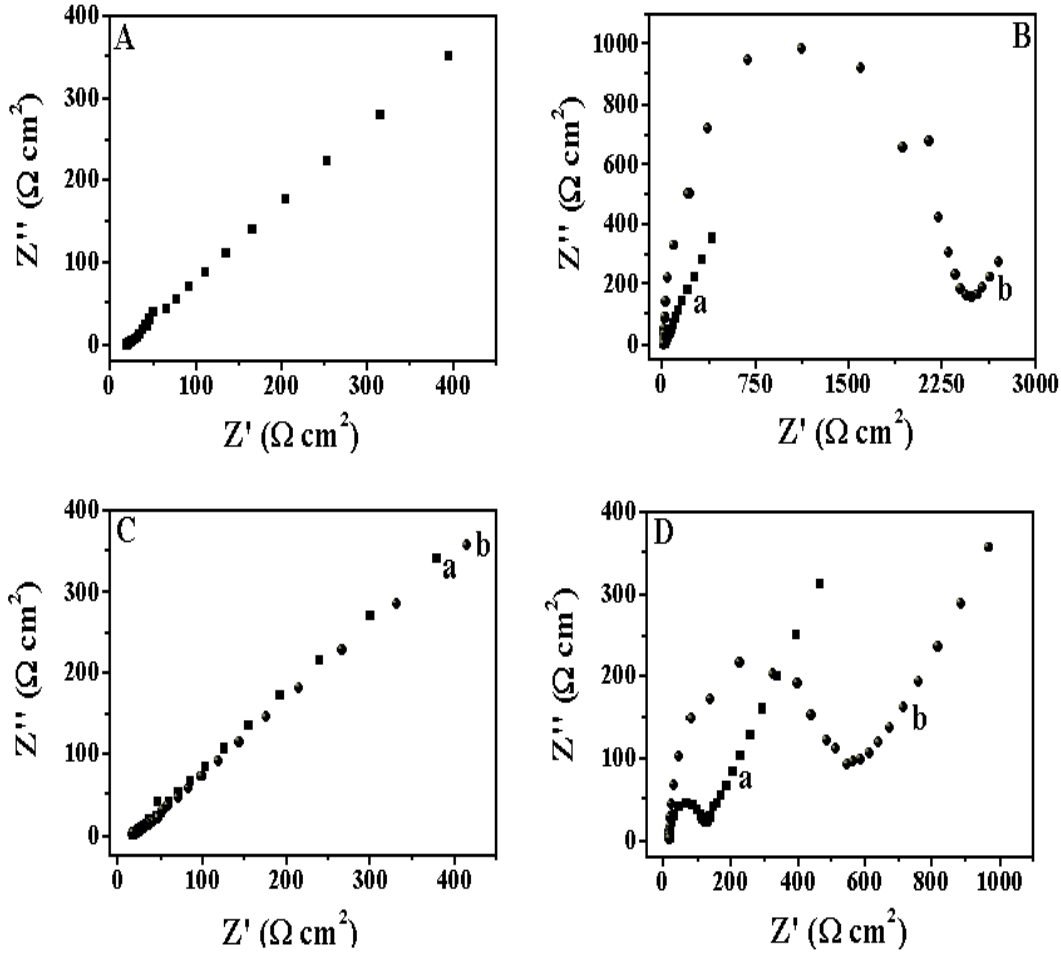

Figure 15: Typical impedance (Nyquist) plots in 1mM hexaammineruthenium(III) chloride with 0.1M lithium perchlorate as a supporting electrolyte for, (A) Bare Au electrode, (B) SAM of TP on Au, (C) SAM of p-ATP on Au and (D) SAM of NT on Au surface respectively. Here (a) represents the monolayer formed from the hexagonal liquid crystalline phase and (b) denotes the monolayer obtained using ethanol as a solvent.

It can be seen from the figure that the bare Au electrode (Fig. 15A) shows a straight line in the entire range of frequency used for the study implying a perfect diffusion controlled process for the redox couple. On the other hand, the SAM of TP on Au obtained using ethanol as a solvent (Fig. 15B (b)) shows a semicircle formation at high frequency region indicating the blocking behaviour of the monolayer towards the redox reaction. But the SAM formed from the hexagonal liquid crystalline phase (Fig. 15B (a)) shows a small semicircle at high frequency region and a straight line at low frequency region indicating a poor blocking property of the SAM. Similarly, it can be noted from the figures 15D (a) and (b) that the SAM of NT on Au surface prepared using both the hexagonal liquid crystalline phase and ethanol shows the formation of semicircle at high frequency region and a straight line at low frequency region indicating the quasi-reversible behaviour for the redox couple, which is the result of poor blocking ability of SAM. The formation of larger semicircle in the case of ethanol adsorbed SAM implies a good blocking ability of SAM towards the diffusion of redox couple when compared to the corresponding SAM formed from the hexagonal liquid crystalline phase. In contrast, the monolayer of p-ATP on Au surface (Fig. 15C) obtained using both the hexagonal liquid crystalline phase (a) and ethanol (b) as adsorbing media shows a straight line in the entire of frequency used for the study indicating a complete diffusion controlled process for the redox reaction of ruthenium complex, which is a result of the poor blocking ability of the SAM. It can also be observed from the figures that the R_{ct} values of SAM formed from ethanol is higher than the one formed from the hexagonal liquid crystalline phase implying a better barrier property and the formation of an ordered, compact SAM with less number of pinholes and defects in the former case. These results are in conformity with our CV results described earlier.

5.6.2. Analysis of impedance data

It is well known that the diameter of semicircle obtained in the impedance plots is a measure of charge transfer resistance (R_{ct}), which quantifies the extent of blocking of the monolayer towards the redox reactions. The charge transfer resistance (R_{ct}) value is higher in the case of SAM modified electrodes when compared to that of the R_{ct} determined at bare Au electrode due to the inhibition of electron transfer rate on the monolayer coated electrodes. The impedance values are fitted to a standard Randle's equivalent circuit comprising of a parallel combination of constant phase element (CPE) represented by Q and a faradaic impedance Z_f in series with the uncompensated solution resistance, R_u. The faradaic impedance, Z_f is a series combination of charge transfer resistance, R_{ct} and the Warburg impedance, W for the cases of bare Au electrode, SAM of p-ATP on Au and SAM of NT on Au (for redox reaction of ruthenium complex) coated electrodes. For the other cases of SAM modified electrodes, the Z_f consists only of charge transfer resistance, R_{ct}. By equivalent circuit fitting procedure using the impedance data of bare Au electrode and aromatic SAM modified electrodes, we have determined the R_{ct} values, which are shown in Table 2. It can be seen from the table that the R_{ct} values of SAM modified electrodes as expected are higher than the bare Au electrode. It can also be seen that the R_{ct} values obtained for the SAMs of TP and p-ATP on Au surface formed from ethanol are higher when compared to the SAMs prepared using the hexagonal liquid crystalline phase implying the better blocking of the SAM to the redox reaction in the former case. In the case of SAM of NT on Au, the R_{ct} value is higher when the hexagonal liquid crystalline phase is used as an adsorbing medium. We have used two different redox probes viz., $[Fe(CN)_6]^{3-|4-}$ and $[Ru(NH_3)_6]^{2+|3+}$ and the R_{ct} values determined using these redox couples for all the aromatic SAM modified

electrodes obtained using both the hexagonal liquid crystalline phase and ethanol as adsorbing media are given in table 2.

Table-2

The charge transfer resistance (R_{ct}) values obtained from the impedance plots of different aromatic SAM modified electrodes using two different redox couples as probe molecules.

Sample	Charge transfer resistance (R_{ct}) values (Ω cm^2)			
	$[Fe(CN)_6]^{3-\|4-}$		$[Ru(NH_3)_6]^{2+\|3+}$	
	Hexagonal LC Phase	Ethanol	Hexagonal LC Phase	Ethanol
TP/Au	7147	24200	13.28	2370
p-ATP/Au	17	114.3	12.78	25
NT/Au	10530	8674	98.46	508.5
Bare Au	1.784		0.6020	

From the R_{ct} values, we have calculated the surface coverage (θ) of these monolayers on the gold electrode using equation (1), by assuming that the current is due to the presence of pinholes and defects within the monolayer.

$$\theta = 1 - (R_{ct}/R'_{ct}) \qquad (1)$$

where R_{ct} is the charge transfer resistance of bare Au electrode and R'_{ct} is the charge transfer resistance of the corresponding SAM modified electrodes. We have determined the surface coverage values of >99.9% for the cases of SAMs of TP and NT coated Au electrodes and 90-98% in the case of SAM of p-ATP on Au surface.

5.6.3. Study of ionic permeability of aromatic SAMs on Au surface

The insulating properties of SAMs have been evaluated by studying the ionic permeation in an inert electrolyte without any redox species using electrochemical impedance spectroscopy. Boubour and Lennox have extensively studied the insulating properties of self-assembled monolayers of n-alkanethiols and ω-functionalized n-alkanethiols using impedance spectroscopy in an inert electrolyte of K_2HPO_4 [42-44]. From the measurement of phase angle at an ion-diffusion-related frequency (1Hz), these authors have classified the SAMs to a pure capacitor ($\geq 88^0$) and a leaky capacitor ($<87^0$) contaminated by a resistive component associated with the current leakage at defect sites. Fawcett et al. [24,25] have studied the ionic permeability of the monolayers of alkanethiol in $NaClO_4$ and tetrapropylammonium perchlorate (TPAP) using impedance spectroscopy and correlated to the structural defects and pinholes in the SAM. In this work, we have used NaF as an inert electrolyte to evaluate the ionic permeability of the SAM modified electrodes. The ionic sizes of Na^+ and F^- ions are smaller compared to previously reported electrolytes. We have used NaF in order to probe the insulating properties of SAM to ionic permeability for very small ions such as Na^+ and F^- ions. We have used impedance spectroscopy as a tool for evaluation at a wider frequency ranging from 100kHz to 0.1Hz.

Figures 16A, B and C show the Bode phase angle plots of SAMs of TP, p-ATP and NT on Au surface in 1M NaF aqueous solution respectively. Insets show the respective total impedance (Z) vs. frequency plots for the corresponding SAM modified electrodes in the same solution. We have compared the insulating properties of these monolayers prepared using both the hexagonal liquid crystalline phase and ethanol as adsorbing media. In all these figures (a) represents the monolayer obtained using the hexagonal liquid

crystalline phase and (b) denotes the corresponding monolayer formed from ethanol as adsorbing media.

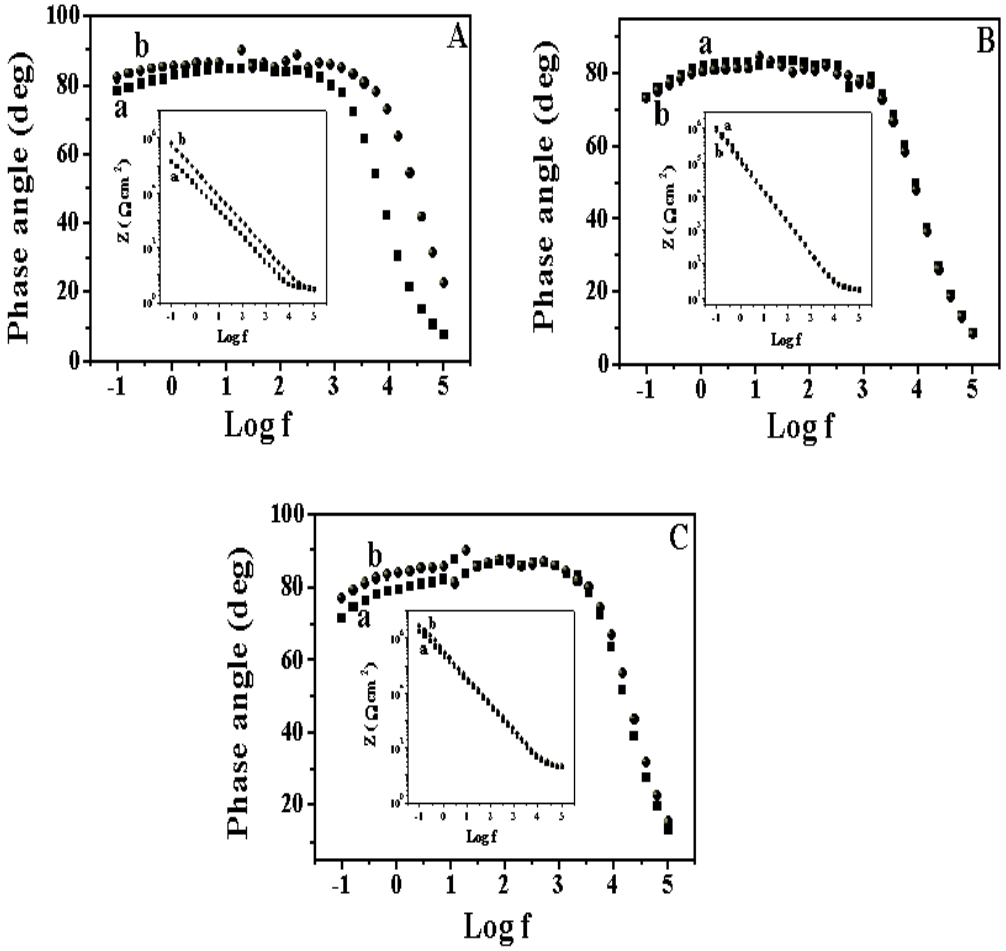

Figure 16: Bode phase angle plots in 1M NaF aqueous solution for (A) SAM of TP on Au, (B) SAM of p-ATP on Au and (C) SAM of NT on Au coated electrodes respectively. Insets show the plots of total impedance (Z) vs. logarithmic frequency for the corresponding SAM modified electrodes. Here (a) represents the monolayer obtained using the hexagonal liquid crystalline phase and (b) denotes the monolayer formed from ethanol as adsorbing media.

It can be seen from the figures that the phase angle values of these aromatic SAMs on Au surface are higher showing more capacitive behaviour, which implies that the ionic permeation is lower and the SAM possesses better insulating properties. This conclusion has been further strengthened by the fact that the total impedance values are higher and the SAM shows a good capacitive behaviour, as can be seen form the insets of the figure 16. In the cases of SAMs of TP (Fig. 16B) and NT (Fig. 16D) on Au surface, the monolayer obtained using ethanol (b) shows a better insulating property when compared to the one formed from the hexagonal liquid crystalline phase (a). This indicates that the monolayer has less ionic permeation and it is structurally ordered in the former case. In the case of p-ATP (Fig. 16C) on Au, there is not much difference in the insulating properties of the monolayers prepared using both the hexagonal liquid crystalline phase (a) and ethanol (b). This implies that these SAMs act as a leaky capacitor contaminated by a resistive component associated with the current leakage at defect sites. The higher phase angle obtained in the case of SAMs prepared from ethanol even at lower frequencies, where ionic permeation is generally favoured, points out to the fact that a compact, dense monolayer has been formed with very low defects. These studies clearly show that the usage of hexagonal liquid crystalline phase as an adsorbing media does not improve the insulating properties of the monolayers of aromatic thiols on Au surface.

Based on the results obtained in the cyclic voltammetry and impedance spectroscopy studies, it has been concluded that the structural integrity and barrier properties of the monolayers of aromatic thiols on Au have not been improved when the hexagonal liquid crystalline phase is used as an adsorbing media. The reason for this may be due to less solubilization of aromatic thiols in the LC phase and there may be some strong interaction between the aromatic

thiols and the surfactant system, which prevents the release of thiol from the hydrophobic core to the gold surface to form a good monolayer. This explanation is a tentative one, which needs to be investigated further. However, the method adopted in this work may still be an effective way of preparing the monolayers in case the aqueous environment is a preferred option or a necessity.

III. SAMs OF ALKOXYCYANOBIPHENYL THIOLS ON GOLD SURFACE

5.7. Introduction

Apart from aliphatic and aromatic thiols, we have also carried out monolayer formation of alkoxycyanobiphenyl thiols on gold surface using the hexagonal lyotropic liquid crystalline phase as an adsorbing medium. The special feature of these alkoxycyanobiphenyl thiols is that it contains both the aliphatic and aromatic parts in its structure. These molecules show a nematic liquid crystalline phase in the bulk sample. It is interesting to study the monolayer formation and its phase behaviour by mixing two different liquid crystalline phases. In the previous chapter, we have discussed about the monolayer formation of these alkoxycyanobiphenyl thiols on gold surface using dichloromethane as a solvent and found that these molecules form a highly dense, well packed, ordered monolayer with less number of defects on gold surface.

Among several aromatic thiols reported in literature, there are some scattered reports on SAM of biphenyl thiol [55-57]. Cyganik et al. reported the scanning tunneling microscopic observation of the influence of spacer chain on the molecular packing of SAMs of ω-biphenylalkanethiols on Au (111) [55].

Long et al. studied the effect of odd-even number of alkyl chains on SAMs of biphenyl-based thiols using cyclic voltammetry [56].

Reports on self-assembled monolayer of molecules, which show the liquid crystalline phase behaviour in bulk are also very rare. In literature, both discotic and calamitic (types of liquid crystalline phases) molecules have been shown to form highly ordered SAMs on gold leading to many interesting properties and phenomena [58-64]. A number of terminally substituted alkoxycyanobiphenyl compounds such as bromo-, hydroxy-, amino-, carboxy-, epoxy- and olefine- terminated cyanobiphenyls are already known. Kumar et al. reported the synthesis of a number of terminal thiol-substituted alkoxycyanobiphenyl compounds [65]. Recently, we have reported the monolayer formation of alkoxycyanobiphenyl thiols on gold surface using dichloromethane as a solvent [66] and found that the redox reaction of ruthenium complex is facilitated by a tunneling process.

In this chapter, we discuss our studies on self-assembled monolayer films of some alkoxycyanobiphenyl molecules functionalized with thiols having different alkyl chain lengths on gold surface using the hexagonal liquid crystalline phase as an adsorbing medium. As described earlier, the liquid crystalline phase behaviour is confirmed by polarizing light microscopy and X-ray diffraction (XRD) studies. Electrochemical techniques such as cyclic voltammetry (CV) and electrochemical impedance spectroscopy (EIS) were used for the evaluation of barrier property of the SAM-modified electrodes using potassium ferrocyanide and hexaammineruthenium(III) chloride complexes as redox probes. Impedance spectroscopy data were used for the calculation of surface coverage and other kinetic parameters for the SAM modified electrodes. We have also compared our results with that of the

corresponding SAMs obtained using dichloromethane as a solvent, which has been described elaborately in the previous chapter.

5.8. Experimental section

5.8.1. Chemicals

Dichloromethane (Spectrochem), Triton X-100 (Spectrochem), potassium ferrocyanide (Loba), potassium ferricyanide (Qualigens), hexaammineruthenium(III) chloride (Alfa Aesar), sodium fluoride (Qualigens) and lithium perchlorate (Acros Organics) were used in this study as received. Alkoxycyanobiphenyl thiol compounds of different chain lengths (C_5(a), C_8(b) and C_{10}(c)) were synthesized by Kumar et al. [65] and the synthetic scheme is described elsewhere [66]. All the chemical reagents used in this work were analytical grade (AR) reagents. Millipore water having a resistivity of 18 MΩ cm was used to prepare the aqueous solutions. The structure of the alkoxycyanobiphenyl thiol compounds studied in this work is shown in the following figure.

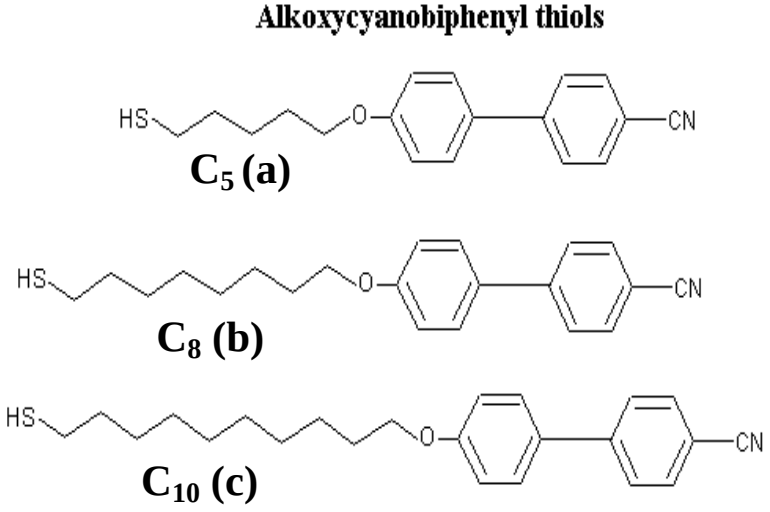

5.8.2. Preparation of the hexagonal liquid crystalline phase

The lyotropic liquid crystalline phase is a mixture of Triton X-100 (42% by weight) and water (58% by weight) [34], which exhibits the broken mosaic and focal conic textures of the hexagonal phase in textural studies using polarizing light microscopy. The hexagonal structure of the liquid crystalline phase is also confirmed by X-ray diffraction studies. For the preparation of SAMs, the alkoxycyanobiphenyl thiol compounds having different chain lengths were added to the above-mentioned liquid crystalline phase. About 5-10 mg of the compound was added to the total volume of 25ml of the hexagonal liquid crystalline phase. Initially, the alkoxycyanobiphenyl compounds were heated to the isotropic phase at respective temperatures into which the liquid crystalline phase consisting of water and Triton X-100 was added and stirred completely to obtain a homogeneous mixture of solution. Then it was allowed to cool down to room temperature and used for the SAM formation. Even after the addition of thiol, the hexagonal structure of the liquid crystalline phase is maintained and it was confirmed by polarizing light microscopy. Although, the alkoxycyanobiphenyl thiol compounds show a nematic phase in the bulk sample, the mixture of a lyotropic liquid crystalline phase and these compounds that has been used for the monolayer preparation shows the hexagonal liquid crystalline phase.

5.8.3. Sample preparation

Gold sample of purity 99.99% was obtained from Arora Mathey, India. Evaporated gold (~100 nm thickness) on glass with chromium underlayers (~ 2-5 nm thickness) was used for the monolayer formation and its characterization using electrochemical techniques. The substrate was heated to 350^0C during gold evaporation under a vacuum pressure of 2 X 10^{-5} mbar, a process that

normally yields a very smooth gold substrate with predominantly Au (111) orientation. The evaporated gold samples were used as strips for SAM formation and its analysis.

For electrochemical characterization, a conventional three-electrode electrochemical cell was used. A platinum foil of large surface area was used as a counter electrode and a saturated calomel electrode (SCE) was used as a reference electrode with the SAM modified gold electrode as a working electrode. The cell was thoroughly cleaned before each experiment and kept in a hot air oven at 100^0C for at least 1 hour before the start of the experiment.

5.8.4. Preparation of alkoxycyanobiphenyl SAMs using the hexagonal liquid crystalline phase

Before SAM formation, the evaporated Au strips were pre-treated with "piranha" solution (It is a mixture of 30% H_2O_2 and Conc. H_2SO_4 in 1:3 ratio) and washed completely with millipore water. The monolayers of alkoxycyanobiphenyl thiols were prepared by keeping the Au strips in the hexagonal liquid crystalline phase containing these thiol molecules for about 15 hours at room temperature. After this, the electrode was thoroughly washed with a jet of distilled water and finally with millipore water. For comparison, we have also prepared the monolayers of alkoxycyanobiphenyl thiols on Au surface using dichloromethane as a solvent. In this case, the Au strips were dipped in 1mM thiol in dichloromethane solution for about 15 hours at room temperature. Upon removal, the SAM coated electrodes were rinsed with dichloromethane, washed with distilled water and finally with millipore water and immediately used for the analysis.

5.8.5. Electrochemical characterization of SAMs on Au surface

Cyclic voltammetry and electrochemical impedance spectroscopy were employed for the characterization of SAM and evaluation of its barrier property by studying the electron transfer reactions on the SAM modified surfaces using two different redox probes namely potassium ferrocyanide (negative redox probe) and hexaammineruthenium(III) chloride (positive redox probe). Cyclic voltammetry was performed in solutions of 10mM potassium ferrocyanide in 1M sodium fluoride at a potential range of –0.1V to 0.5V vs. SCE and 1mM hexaammineruthenium(III) chloride in 0.1M lithium perchlorate at a potential range of –0.4V to 0.1V vs. SCE. The impedance measurements were carried out using an ac signal of 10mV amplitude at a formal potential of the redox couple using a wide frequency range of 100kHz to 0.1Hz, in solution containing always equal concentrations of both the oxidized and reduced forms of the redox couple namely, 10mM potassium ferrocyanide and 10mM potassium ferricyanide in 1M NaF. All the experiments were performed at room temperature.

5.8.6. Instrumentation

Cyclic voltammetry was carried out using an EG&G potentiostat (model 263A) interfaced to a computer through a GPIB card (National Instruments). The potential ranges and scan rates used are shown in the respective diagrams. For electrochemical impedance spectroscopic studies the potentiostat was used along with an EG&G 5210 lock-in-amplifier controlled by Power Sine software. The electrochemical impedance spectroscopy data were used for the equivalent circuit fitting analysis using Zsimpwin software (EG&G) developed on the basis of Boukamp's model. Based on this procedure, the charge transfer resistance values (R_{ct}) of SAM modified electrodes were calculated, from which

the surface coverage (θ) values of these monolayers on gold surface were also determined.

5.9. Results and discussion

5.9.1. Polarizing light microscopy

The polarizing light microscopy is a very simple and inexpensive experimental technique, which can be used to identify the various mesophases formed by the self-assembly of surfactants. The experiments were conducted using glass slides and cover slips with the sample sandwiched between them. The textural studies were carried out by heating the sample to isotropic phase using Mettler heating arrangement and recording the textures during the process of cooling. We have observed broken focal conic textures [35] and striations [36] corresponding to the hexagonal structure of the liquid crystalline phase for solutions containing in addition to Triton X-100/water, alkoxycyanobiphenyl thiols. These textural studies confirm the hexagonal structure of the liquid crystalline phase used for the preparation of monolayer and the results are similar to that described in the previous section.

5.9.2. Electrochemical characterization

5.9.2.1. Cyclic voltammetry

Cyclic voltammetry is an important tool to assess the quality of the monolayer and its barrier property by studying the electron transfer reaction of redox probe molecule on the SAM modified surfaces. The SAMs of alkoxycyanobiphenyl thiols on gold surface were formed from the hexagonal liquid crystalline phase containing the respective thiol molecule. For comparison the corresponding monolayers obtained using dichloromethane as a solvent were also characterized. Figure 17A shows the cyclic voltammograms

of bare Au electrode and SAMs of alkoxycyanobiphenyl thiols coated Au electrodes in 10mM potassium ferrocyanide with 1M NaF as the supporting electrolyte at a potential scan rate of 50mV/s. Figure 17B shows the comparison of cyclic voltammograms of monolayers of alkoxycyanobiphenyl thiols having different chain lengths coated Au electrodes in the same solution. The monolayers were formed by keeping the Au strips in the corresponding thiol solution for about 15 hours. It can be seen from the figure that the bare Au electrode (Fig. 17A (a)) shows a perfect reversible voltammogram for the redox couple indicating that the electron transfer reaction is completely diffusion controlled. In contrast, the monolayers of all the alkoxycyanobiphenyl thiol-coated electrodes (Fig. 17A (b)) do not show any peak formation as the redox reaction is completely blocked by the monolayer. They exhibit the characteristics of microelectrode array behaviour.

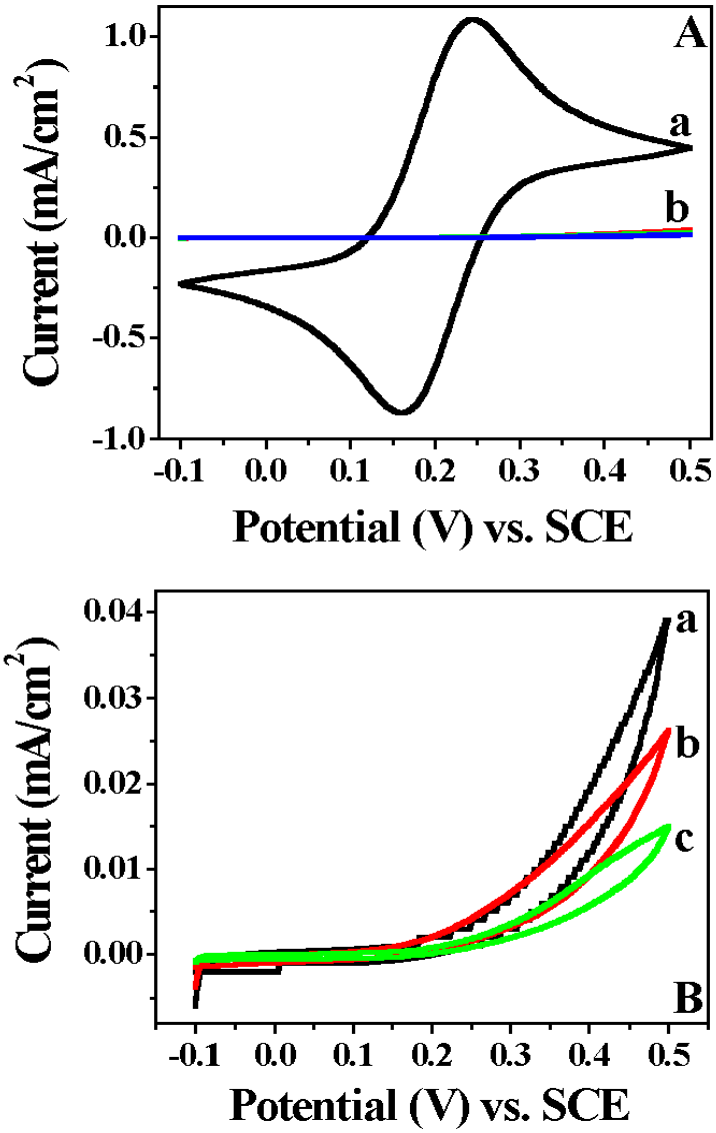

Figure 17: Cyclic voltammograms of 10mM potassium ferrocyanide with 1M NaF as supporting electrolyte at a potential scan rate of 50mV/s for, (A) Bare gold electrode (a) and SAMs of alkoxycyanobiphenyl thiols on Au formed from the hexagonal liquid crystalline phase (b) for about 15hours. (B) Comparison of cyclic voltammograms of SAMs of C_5 (a), C_8 (b) and C_{10} (c) thiols on gold surface formed from the hexagonal liquid crystalline phase for about 15 hours in the same solution.

Figure 17B shows the comparison of cyclic voltammograms of alkoxycyanobiphenyl thiols having different alkyl chain lengths namely C_5 (a), C_8 (b) and C_{10} (c) thiols formed from the hexagonal liquid crystalline phase by keeping the Au strips for about 15 hours. It can be seen from the figure that all the monolayer coated electrodes show a complete blocking to the redox reaction indicating the charge transfer control for the electron transfer reactions on these electrodes. The blocking ability of these monolayers follows the order: $C_{10} > C_8 > C_5$. These monolayers on Au surface exhibit the microelectrode array behaviour indicating the formation of highly ordered, well packed monolayers with less number of pinholes and defects.

We have compared the blocking ability of these monolayers formed from the hexagonal liquid crystalline phase with that of the corresponding monolayers prepared using dichloromethane as a solvent. Figure 18 shows the comparison of cyclic voltammograms of respective SAM modified electrodes obtained using the hexagonal liquid crystalline phase and dichloromethane as adsorbing medium. Figures 18A, B and C show the cyclic voltammograms in 10mM potassium ferrocyanide with 1M NaF as supporting electrolyte at a potential scan rate of 50 mV/s for C_5, C_8 and C_{10} thiols respectively. In these figures, (a) denotes the monolayer formed from the hexagonal liquid crystalline phase and (b) represents the corresponding monolayer obtained using dichloromethane as a solvent. It can be seen from the figures that the monolayers formed from the hexagonal liquid crystalline phase (a) exhibit a more blocking characteristic than the one formed from dichloromethane (b). The magnitude of current is much lower at a positive potential range of >0.1V vs. SCE in the case of SAMs formed from the hexagonal liquid crystalline phase, when compared to the corresponding monolayers formed using dichloromethane as a solvent. This clearly shows that the SAMs formed from

the hexagonal liquid crystalline phase have a better blocking property and are highly ordered and compact with ultra-low defect density. The small current flow arises due to the access of the redox species to the gold surface through the pinholes and defects present in the monolayer.

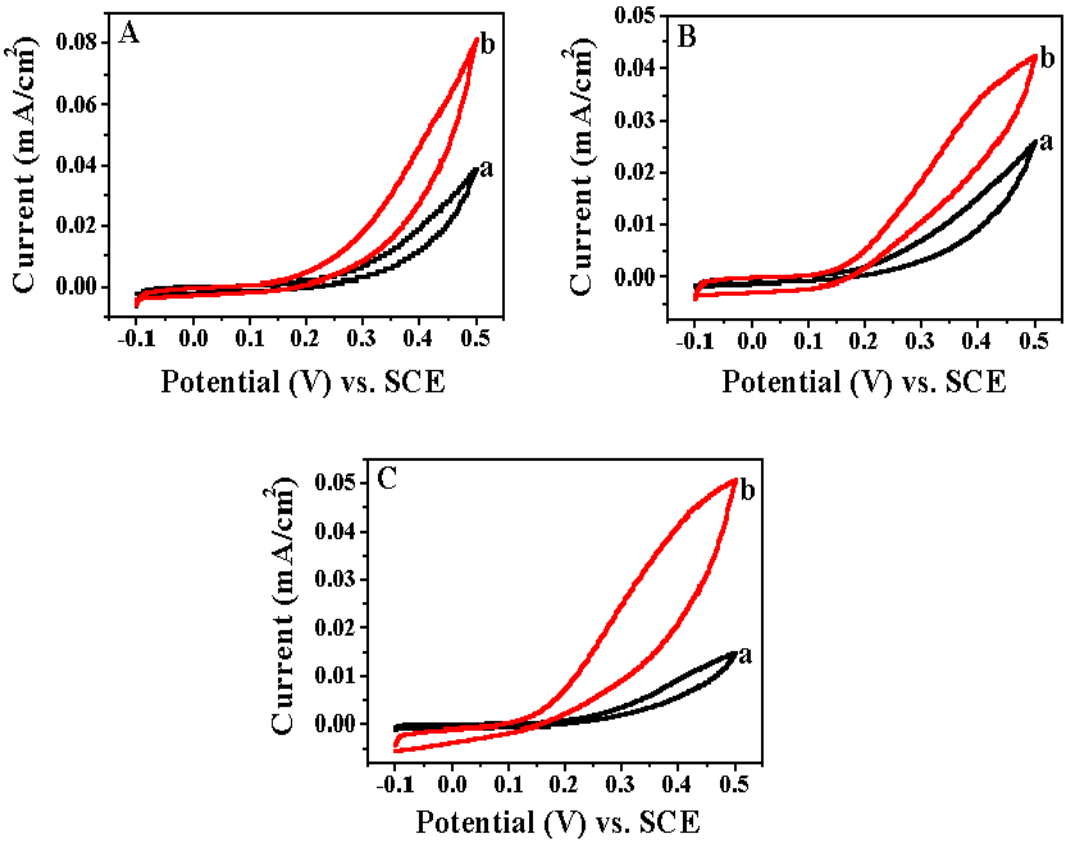

Figure 18: Comparison of cyclic voltammograms in 10mM potassium ferrocyanide with 1M NaF as supporting electrolyte at a potential scan rate of 50 mV/s for, (A) C_5, (B) C_8 and (C) C_{10} alkoxycyanobiphenyl thiols respectively. Here (a) denotes the SAMs formed from the hexagonal liquid crystalline phase and (b) represents the corresponding SAMs obtained using dichloromethane as a solvent.

We have also used hexaammineruthenium(III) chloride as a redox probe molecule to evaluate the barrier property of the monolayers of alkoxycyanobiphenyl thiols on Au surface obtained using both the hexagonal liquid crystalline phase and dichloromethane as adsorbing media. Figure 19 shows the CVs obtained for bare gold and SAMs of alkoxycyanobiphenyl thiols modified Au electrodes using the hexagonal liquid crystalline phase in 1mM hexaammineruthenium(III) chloride with 0.1M lithium perchlorate as the supporting electrolyte at a potential scan rate of 50mV/s. The monolayers were formed by keeping the Au sample in the corresponding thiol for about 15 hours. It can be observed from the figure that the bare Au electrode (Fig. 19(a)) shows the reversible voltammogram indicating that the ruthenium redox reaction is completely diffusion controlled. It can be seen from Fig. 19(b) that the redox reaction is quasi-reversible implying very poor blocking property of the SAM of C_5 thiol on Au surface. In contrast, the monolayers of C_8 (c) and C_{10} (d) thiols formed from the hexagonal liquid crystalline phase show a complete blocking behaviour with no peak formation to ruthenium electron transfer reaction exhibiting the characteristic of an array of microelectrodes. It is clear from the figure that the monolayer of C_{10} alkoxycyanobiphenyl thiol (d) shows the perfect blocking behaviour to the redox reaction with almost defect free structure when compared to other monolayers on gold surface and the blocking efficiency follows the order: $C_{10} > C_8 > C_5$. These results indicate the formation of highly compact, well packed, ordered monolayers of alkoxycyanobiphenyl thiols on gold surface obtained using the hexagonal liquid crystalline phase as an adsorbing medium.

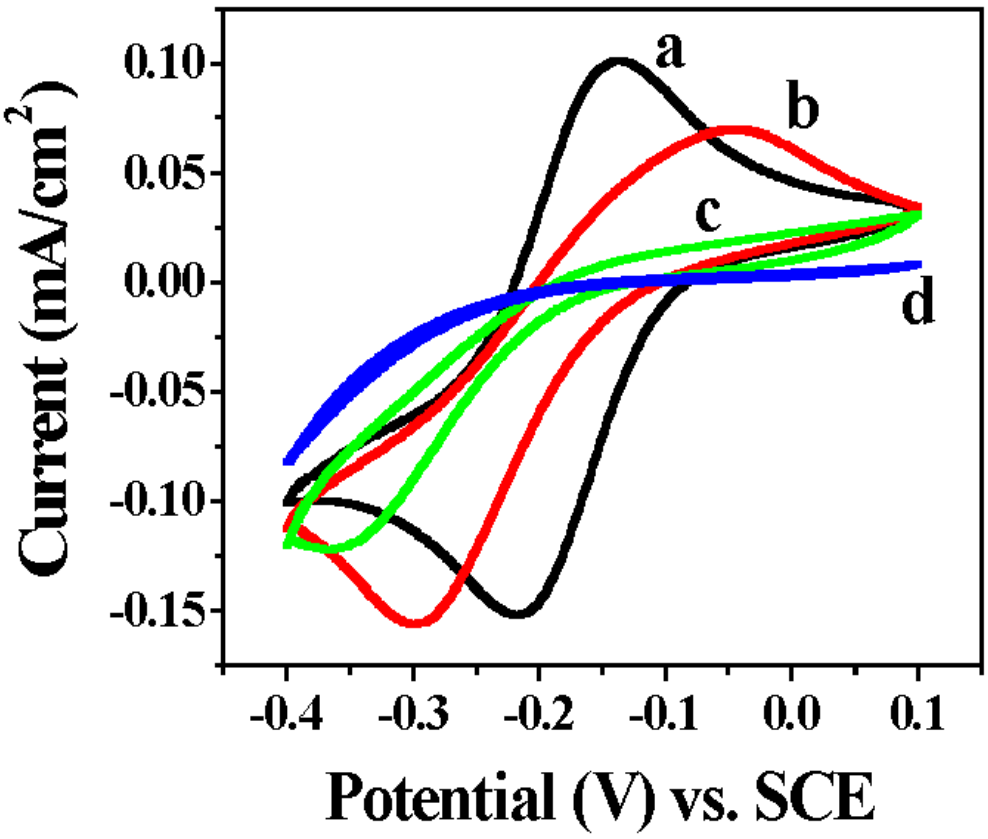

Figure 19: Cyclic voltammograms of 1mM hexaammineruthenium(III) chloride with 0.1M $LiClO_4$ as the supporting electrolyte at a potential scan rate of 50mV/s for, (a) Bare Au electrode, (b), (c) and (d) are the SAMs of alkoxycyanobiphenyl thiols having alkyl chain lengths C_5, C_8 and C_{10} respectively formed from the hexagonal liquid crystalline phase by keeping the Au strips for about 15 hours.

We have compared the blocking ability of these monolayers formed from the hexagonal liquid crystalline phase with that of the corresponding monolayers prepared using dichloromethane as a solvent. In this case ruthenium complex is used as a redox probe. Figure 20 shows the comparison of cyclic voltammograms of respective SAM modified electrodes obtained using the hexagonal liquid crystalline phase and dichloromethane as adsorbing medium. Figures 20A, B and C show the cyclic voltammograms in 1mM hexaammineruthenium(III) chloride with 0.1M $LiClO_4$ as the supporting electrolyte at a potential scan rate of 50 mV/s for C_5, C_8 and C_{10} alkoxycyanobiphenyl thiols respectively. In these figures, (a) denotes the monolayer formed from the hexagonal liquid crystalline phase and (b) represents the corresponding monolayer obtained using dichloromethane as a solvent. It can be seen from the figures that the monolayers in the case of C_5 (A) and C_8 (B) thiols do not show much difference in their blocking ability to the ruthenium redox reaction when these monolayers formed from either the hexagonal liquid crystalline phase (a) or dichloromethane (b) as adsorbing media. But the monolayer of C_{10} thiol (C) formed from the hexagonal liquid crystalline phase (a) exhibit a more complete blocking characteristics than the one formed from dichloromethane (b). It can also be observed from the figure that the monolayer of C_{10} thiol formed from dichloromethane (b) shows a complete diffusion controlled process for the redox reaction. This is due to the intercalation of solvent molecules during the adsorption process (for a long time), which ultimately disorganizes the monolayer by solvating the thiol molecules and this effect is predominant in the case of longer alkyl chain molecules like C_{10} thiol. The magnitude of current is relatively lower in the case of SAMs formed from the hexagonal liquid crystalline phase, when compared to the corresponding monolayers formed using dichloromethane as a solvent.

This clearly shows that the SAMs formed from the hexagonal liquid crystalline phase have a better blocking property and are highly ordered and compact with ultra-low defect density when compared to the corresponding SAMs obtained using dichloromethane as a solvent. In the case of adsorption in the hexagonal liquid crystalline phase, the organization of the alkyl chains is significantly improved by the aqueous environment and polar end groups of the cylindrical micelles neighbouring the substrate.

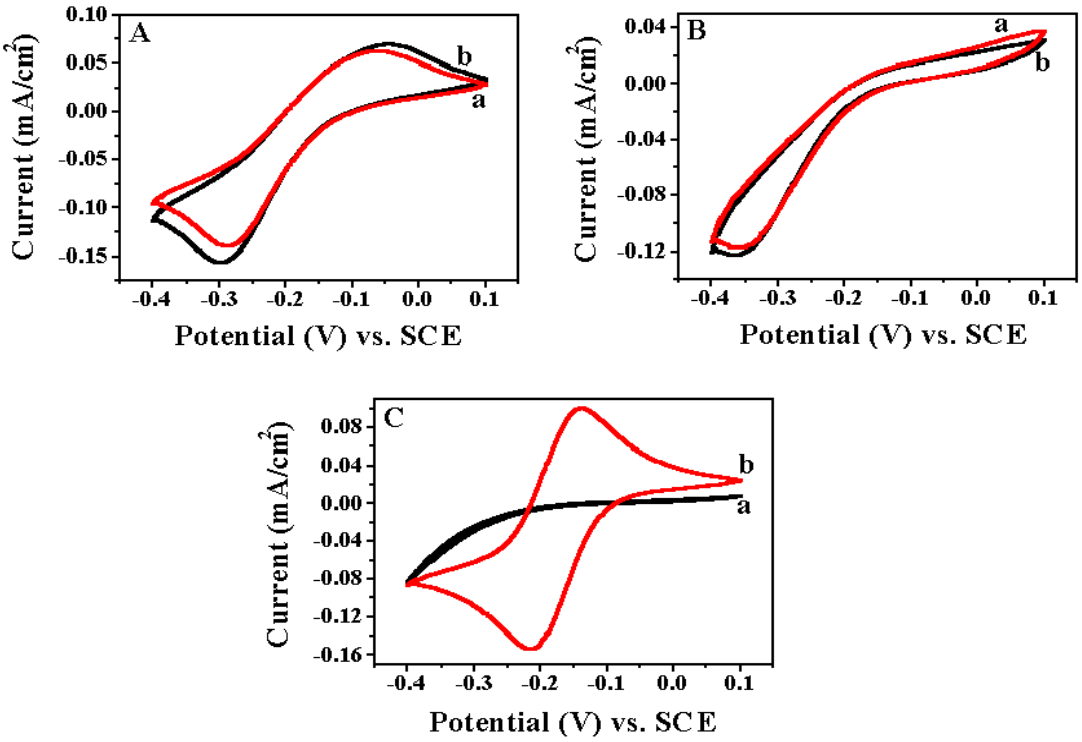

Figure 20: Comparison of cyclic voltammograms in 1mM hexaammineruthenium(III) chloride with 0.1M $LiClO_4$ as the supporting electrolyte at a potential scan rate of 50 mV/s for, (A) C_5, (B) C_8 and (C) C_{10} alkoxycyanobiphenyl thiols respectively. Here (a) denotes the SAMs formed from the hexagonal liquid crystalline phase and (b) represents the corresponding SAMs obtained using dichloromethane as a solvent.

5.9.2.2. Electrochemical impedance spectroscopy

In order to evaluate the structural integrity of the monolayer formed from the hexagonal liquid crystalline phase in a quantitative manner, the charge transfer resistances of the SAM modified electrodes against the diffusion of the redox probe were measured using electrochemical impedance spectroscopy. In addition the impedance data were also used to determine the surface coverage of these monolayers on gold surface. Figure 21B shows the impedance plots (Nyquist plots) of the monolayers of alkoxycyanobiphenyl thiols on Au surface in equal concentrations of potassium ferro/ferri cyanide with NaF as the supporting electrolyte. The monolayers were obtained by keeping the Au strips in the corresponding thiol solution for about 15 hours. For comparison the plot of bare Au electrode was also shown in the Figure 21A. The impedance spectroscopy was carried out at a formal potential of $[Fe(CN)_6]^{3-|4-}$ redox couple. It can be seen from the figure that the bare Au electrode (Fig. 21A) shows a very small semicircle at high frequency region and a straight line at low frequency region indicating that the electron transfer process of the redox couple is essentially diffusion controlled. On the other hand, the SAM modified electrodes (Fig. 21B) show the formation of semicircle in the entire range of frequency used for the study implying a perfect blocking behaviour and complete charge transfer control for the electron transfer process. Figure 21B shows the impedance plots of monolayers of C_5 (a), C_8 (b) and C_{10} (c) thiols on Au surface respectively. A very large semicircle obtained in the case of SAM of C_{10} thiol on Au surface formed from the hexagonal liquid crystalline phase (Fig. 21B (c)) when compared to other SAMs indicates an excellent electrochemical blocking ability of the SAM with the higher charge transfer resistance against the diffusion of redox probe.

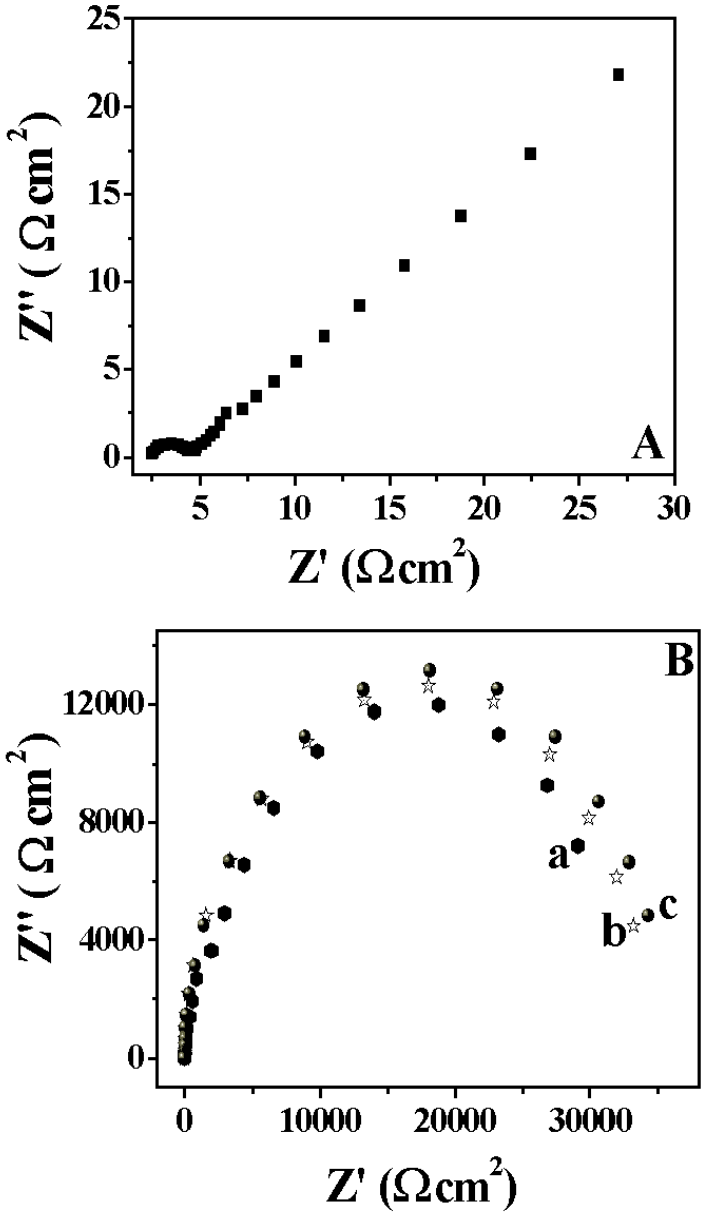

Figure 21: The impedance (Nyquist) plots in 10mM potassium ferrocyanide and 10mM potassium ferricyanide with 1M NaF as the supporting electrolyte for, (A) Bare Au electrode. (B) SAMs of alkoxycyanobiphenyl thiols with different alkyl chain lengths of C_5 (a), C_8 (b) and C_{10} (c) formed using the hexagonal liquid crystalline phase respectively.

Figure 22 shows the comparison of impedance plots of alkoxycyanobiphenyl thiols prepared from the hexagonal liquid crystalline phase and dichloromethane as adsorbing media. Figures 22A, B and C show the respective Nyquist plots of SAMs of C_5, C_8 and C_{10} thiols on Au surface and in all these figures (a) denotes the monolayer formed from dichloromethane as a solvent and (b) stands for the monolayer obtained using the hexagonal liquid crystalline phase.

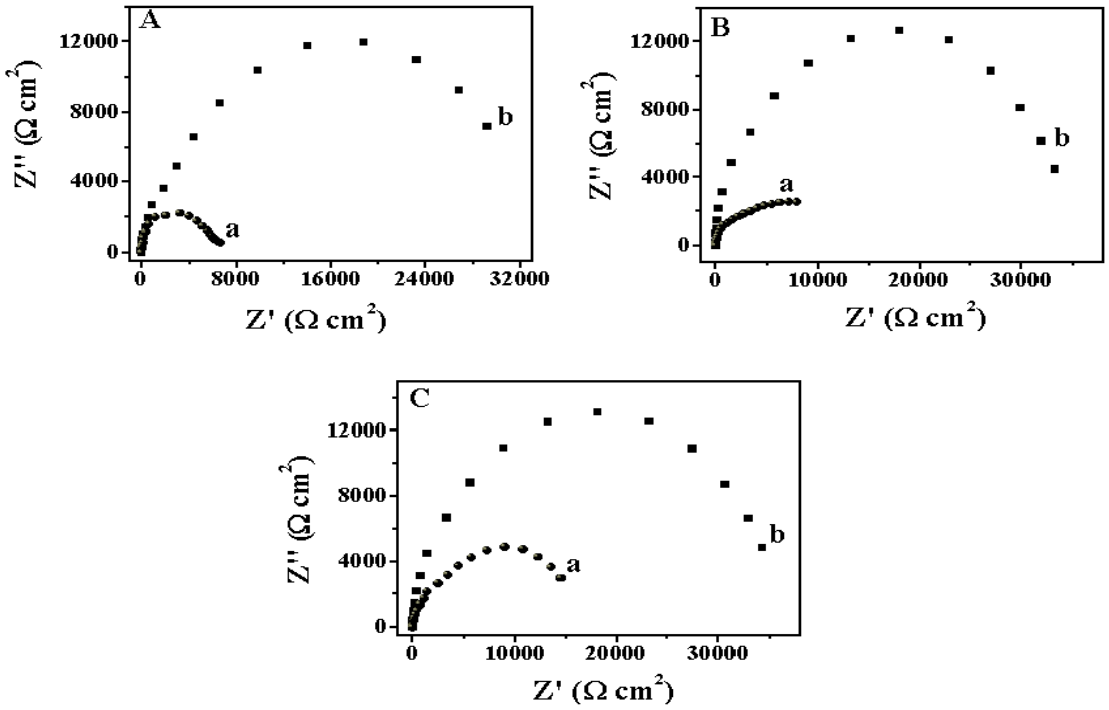

Figure 22: Impedance plots in 10mM potassium ferrocyanide and 10mM potassium ferricyanide with 1M NaF as supporting electrolyte for SAMs of alkoxycyanobiphenyl thiols having different alkyl chain lengths of C_5 (A), C_8 (B) and C_{10} (C) on Au surface respectively. Here (a) denotes the SAM formed from dichloromethane as a solvent and (b) represents the monolayer obtained using the hexagonal liquid crystalline phase.

It is well known that the charge transfer resistance (R_{ct}), which is a measure of the blocking ability of the monolayer, can be determined from the semicircle obtained in the impedance plot. It can be seen from the figures that the R_{ct} values of the monolayers formed from the liquid crystalline phase (b) is much higher than the one formed from dichloromethane as a solvent (a) implying that a highly ordered, well packed, compact monolayer with less number of pinholes and defects is formed in the former case.

Figures 23A and B show the respective Nyquist plots of bare Au electrode and SAMs of alkoxycyanobiphenyl thiols on Au electrodes in 1mM hexaammineruthenium(III) chloride with 0.1M $LiClO_4$ as the supporting electrolyte. The monolayers were formed by keeping the Au sample in the corresponding thiol for about 15 hours. It can be seen from the figure that the bare Au electrode (Fig. 23A) shows a straight line in the entire range of frequency used for the study implying a perfect diffusion controlled process for the ruthenium redox couple. Figure 23B shows the respective impedance plots of SAMs of C_5 (a), C_8 (b) and C_{10} (c) alkoxycyanobiphenyl thiols on Au surface obtained using the hexagonal liquid crystalline phase. It can be noted from the Fig. 23B (a) that the SAM of C_5 thiol shows the formation of semicircle at high frequency region and a straight line at low frequency region indicating the quasi-reversible behaviour for the redox couple implying a poor blocking ability of SAM. Figures 23B (b) and (c) show the formation of larger semicircle almost in the entire range frequency implying a good blocking ability of the SAMs of C_8 (b) and C_{10} (c) thiols on Au surface towards the diffusion of redox couple. The R_{ct} values increase in the order $C_5 < C_8 < C_{10}$, which indicates the increasing order of blocking efficiency of these monolayers on Au surface.

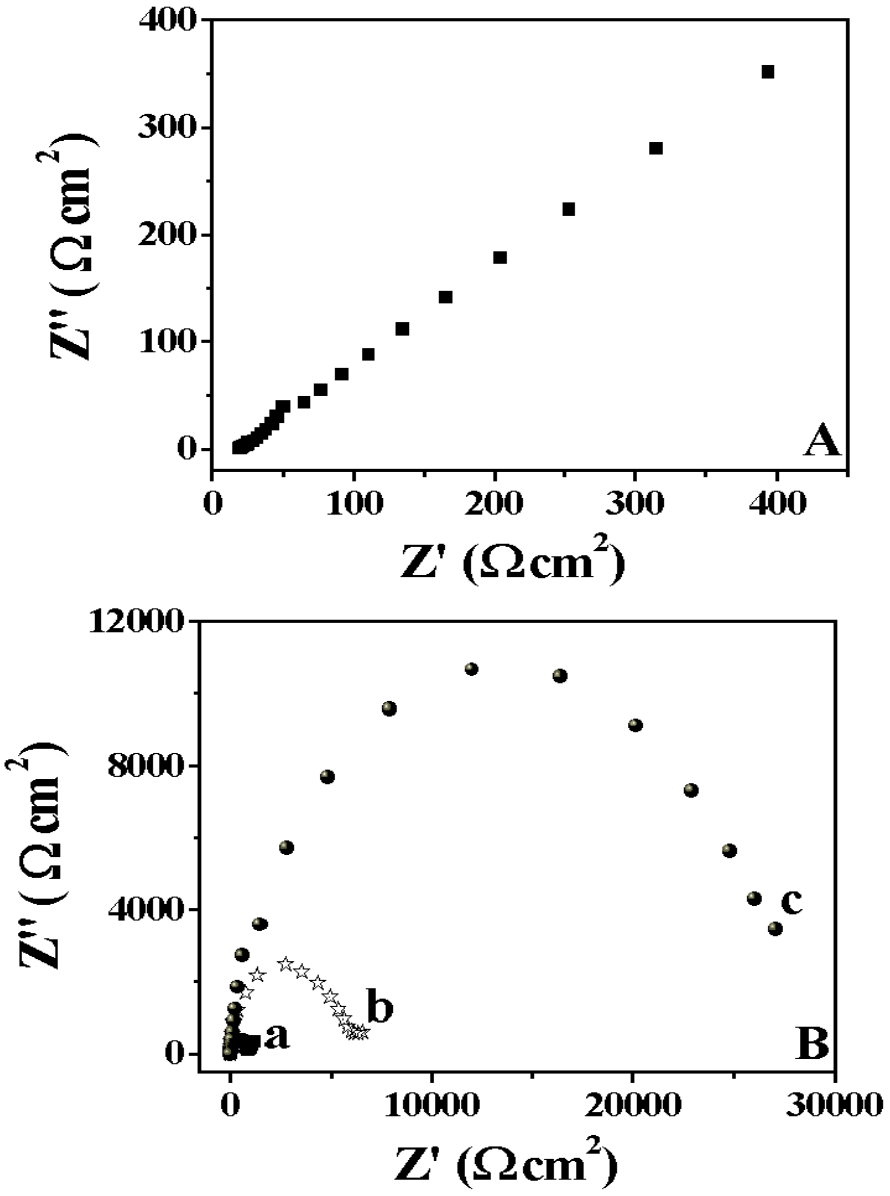

Figure 23: The impedance (Nyquist) plots in 1mM hexaammineruthenium(III) chloride with 0.1M $LiClO_4$ as the supporting electrolyte for, (A) Bare Au electrode. (B) SAMs of alkoxycyanobiphenyl thiols with different alkyl chain lengths of C_5 (a), C_8 (b) and C_{10} (c) formed using the hexagonal liquid crystalline phase respectively.

Figure 24 shows the comparison of impedance plots of alkoxycyanobiphenyl thiols prepared from the hexagonal liquid crystalline phase and dichloromethane as adsorbing media in 1mM hexaammineruthenium(III) chloride with 0.1M lithium perchlorate as the supporting electrolyte. Figures 24A, B and C show the respective Nyquist plots of SAMs of C_5, C_8 and C_{10} thiols on Au surface and in all these figures (a) denotes the monolayer formed from dichloromethane as a solvent and (b) stands for the monolayer obtained using the hexagonal liquid crystalline phase.

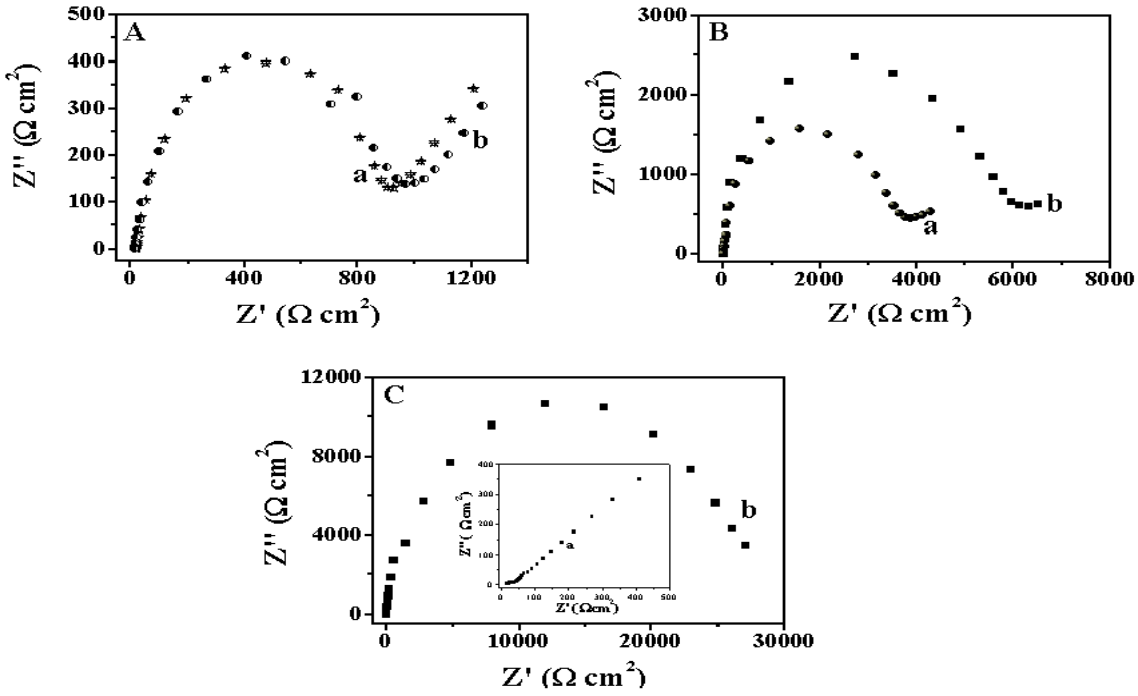

Figure 24: Impedance plots in 1mM hexaammineruthenium(III) chloride with 0.1M $LiClO_4$ as the supporting electrolyte for SAMs of alkoxycyanobiphenyl thiols having different alkyl chain lengths of C_5 (A), C_8 (B) and C_{10} (C) on Au surface respectively. Here (a) denotes the SAM formed from dichloromethane as a solvent and (b) represents the monolayer obtained using the hexagonal liquid crystalline phase. Inset shows the figure (a) for C_{10} thiol.

It can be seen from the figures that the R_{ct} values of the monolayers formed from the liquid crystalline phase (b) is higher than the one formed from dichloromethane as a solvent (a) and this effect is very clear in the case of C_{10} thiol (C) where the solvent adsorbed monolayer (See the inset of figure C) shows a diffusion controlled process for the electron transfer reaction due to the intercalation of solvent molecules in the monolayer film that ultimately disorganizes the monolayer. This implies that a highly ordered, well-packed, compact monolayer with less number of pinholes and defects is formed in the hexagonal liquid crystalline phase when compared to the monolayers obtained using dichloromethane as a solvent. These results are in conformity with our CV results discussed earlier.

5.9.2.3. Analysis of impedance data

It is well known that the diameter of semicircle obtained in the impedance plots is a measure of charge transfer resistance (R_{ct}), which is higher in the case of SAM modified electrodes when compared to that of the corresponding R_{ct} determined at bare Au electrode due to the inhibition of electron transfer rate on the monolayer coated electrodes. The impedance values are fitted to a standard Randle's equivalent circuit comprising of a parallel combination of constant phase element (CPE) represented by Q and a faradaic impedance Z_f in series with the uncompensated solution resistance, R_u. The faradaic impedance, Z_f is a series combination of charge transfer resistance, R_{ct} and the Warburg impedance, W for the cases of bare Au electrode and SAM of C_5 thiol on Au (for redox reaction of ruthenium complex) coated electrode. For the other cases of SAM modified electrodes, the Z_f consists only of charge transfer resistance, R_{ct}. By equivalent circuit fitting procedure using the impedance data of bare Au electrode and SAM modified electrodes, we have

determined the R_{ct} values, which are shown in Table 3. It can be seen from the table that the R_{ct} values of SAM modified electrodes as expected are several orders of magnitude higher than the bare Au electrode. It can also be seen that the R_{ct} values obtained for the SAMs formed from the hexagonal liquid crystalline phase are very much higher when compared to the SAMs formed from dichloromethane implying the better blocking ability of the SAM to the redox reaction in the former case. We have used two different redox probes viz., $[Fe(CN)_6]^{3-|4-}$ and $[Ru(NH_3)_6]^{2+|3+}$ and the R_{ct} values determined using these redox couples for all the SAM modified electrodes obtained using both the hexagonal liquid crystalline phase and dichloromethane as adsorbing media are given in table 3.

Table-3

The charge transfer resistance (R_{ct}) values obtained from the impedance plots of different SAM modified electrodes using two different redox couples as probe molecules.

Sample	Charge transfer resistance (R_{ct}) values (Ω cm^2)			
	$[Fe(CN)_6]^{3-\|4-}$		$[Ru(NH_3)_6]^{2+\|3+}$	
	Hexagonal LC Phase	Dichloromethane	Hexagonal LC Phase	Dichloromethane
C_5 thiol/Au	29230	5980	912.7	857.7
C_8 thiol/Au	31730	6713	5600	3556
C_{10} thiol/Au	36650	13080	27010	21.11
Bare Au	1.784		0.6020	

From the R_{ct} values, we have calculated the surface coverage (θ) of the monolayers of alkoxycyanobiphenyl thiols on the gold electrode using equation (1), by assuming that the current is due to the presence of pinholes and defects within the monolayer.

$$\theta = 1 - (R_{ct}/R'_{ct}) \quad (1)$$

where R_{ct} is the charge transfer resistance of bare Au electrode and R'_{ct} is the charge transfer resistance of the corresponding SAM modified electrodes. The surface coverage values are >99.9% for all the SAM coated electrodes studied in this work and the corresponding values are shown in table 4. From the calculated R_{ct} values, it is clear that the higher alkyl chain containing alkoxycyanobiphenyl thiols form a better blocking monolayer and the extent of blocking follows the order, $C_{10} > C_8 > C_5$, which is in conformity with our CV results discussed earlier. From the R_{ct} and surface coverage values given in the tables 3 and 4, we conclude that the SAMs of alkoxycyanobiphenyl thiols on Au surface obtained using the hexagonal liquid crystalline phase have better blocking ability and highly ordered, compact with ultra low defects when compared to the corresponding SAMs formed from dichloromethane as a solvent.

Table-4

The surface coverage (θ) values calculated using R_{ct} values obtained from the impedance plots of different SAM modified electrodes using two redox probes.

Sample	Surface coverage (θ) values	
	$[Fe(CN)_6]^{3-\|4-}$	$[Ru(NH_3)_6]^{2+\|3+}$
C_5 thiol/Au	**0.9999**	**0.9994**
C_8 thiol/Au	**0.9999**	**0.9999**
C_{10} thiol/Au	**0.9999**	**0.9999**

5.9.2.4. Study of ionic permeability of SAMs of alkoxycyanobiphenyl thiols on gold surface

The insulating properties of SAM have been evaluated by studying the ionic permeation in an inert electrolyte without any redox species using electrochemical impedance spectroscopy. Boubour and Lennox have extensively studied the insulating properties of self-assembled monolayers of n-alkanethiols and ω-functionalized n-alkanethiols using impedance spectroscopy in an inert electrolyte of K_2HPO_4 [42-44]. From the measurement of phase angle at an ion-diffusion-related frequency (1Hz), these authors have classified the SAMs to a pure capacitor ($\geq 88^0$) and a leaky capacitor ($<87^0$) contaminated by a resistive component associated with the current leakage at defect sites. Fawcett et al. [24,25] have studied the ionic permeability of the monolayers of alkanethiol in $NaClO_4$ and tetrapropylammonium perchlorate (TPAP) using impedance spectroscopy and correlated to the structural defects and pinholes in the SAM. In this work, we have used NaF as an inert electrolyte to evaluate the ionic permeability of the SAMs of alkoxycyanobiphenyl thiols on Au surface. The ionic sizes of Na^+ and F^- ions are smaller compared to the sizes of previously reported electrolytes. We have used NaF in order to probe the insulating properties of these SAMs to ionic permeability for very small ions such as Na^+ and F^- ions. We have used impedance spectroscopy as a tool for evaluation at a wider frequency ranging from 100kHz to 0.1Hz.

Figure 25A shows the Bode phase angle plots of SAMs of alkoxycyanobiphenyl thiols having different chain lengths namely C_{10} (a), C_8 (b) and C_5 (c) respectively obtained using the hexagonal liquid crystalline phase as an adsorbing medium in 1M NaF solution without any redox species. The monolayers were formed by keeping the Au strips in the corresponding thiol solution for about 15 hours.

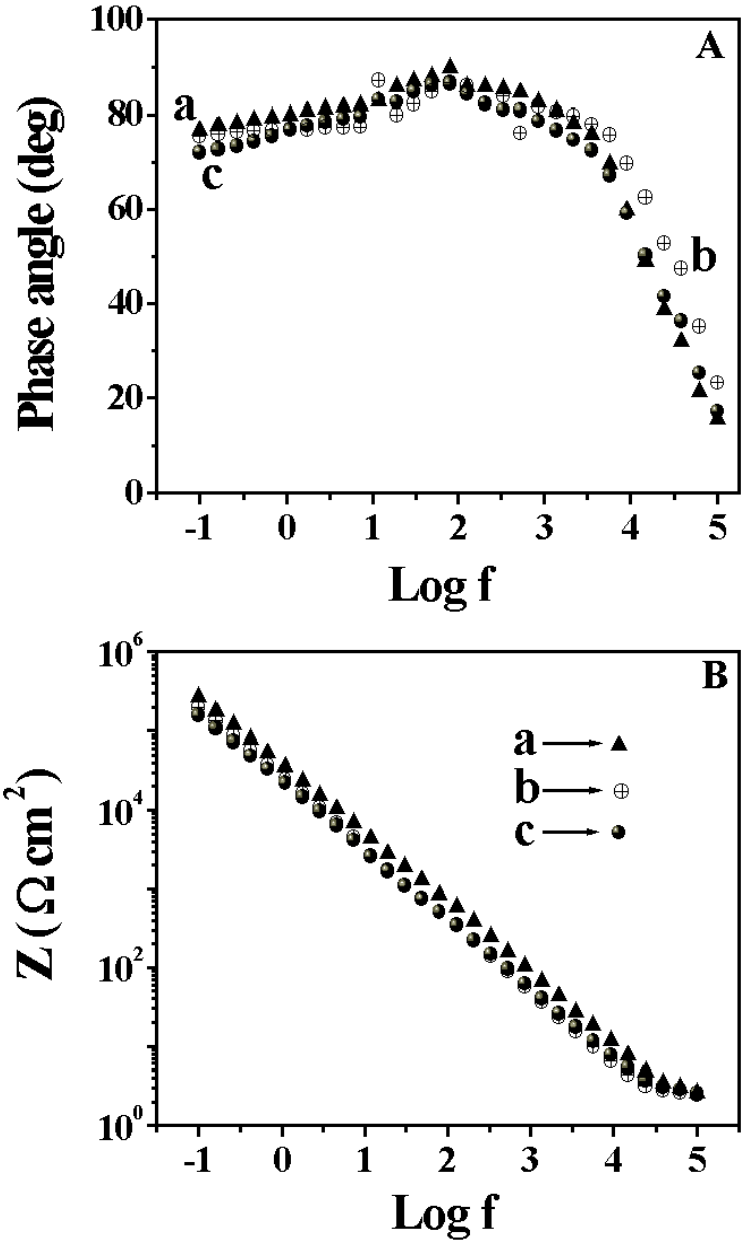

Figure 25: (A) Bode phase angle plots in 1M NaF aqueous solution for (a) SAM of C_{10} thiol, (b) SAM of C_8 thiol and (c) SAM of C_5 thiol on Au surface prepared using the hexagonal liquid crystalline phase as an adsorbing medium. (B) Plots of total impedance (Z) vs. logarithmic frequency for the above-mentioned SAM modified electrodes.

It can be seen from the figures that the phase angle values of these SAMs are higher and it follows the order $C_{10} > C_8 > C_5$. This implies that the ionic permeation is lower and the SAM possesses better insulating properties when the alkyl chain length is longer. This conclusion has been further strengthened by the fact that the impedance values are higher and the SAM shows a capacitive behaviour, as can be seen form the figure 25B. We have obtained a phase angle of 80^0, 77^0 and 76^0 at 1Hz and 77^0, 75^0 and 72^0 at 0.1Hz for the respective SAMs of C_{10} (a), C_8 (b) and C_5 (c) on Au obtained using the hexagonal liquid crystalline phase as a solvating medium. This implies that these SAMs act as a leaky capacitor contaminated by a resistive component associated with the current leakage at defect sites. The corresponding total impedance values as a function of logarithmic frequency for these SAMs are shown in figure 25B. It can be noted from the figures that the total impedance values are higher and there is a very little difference in the impedance values among the different alkyl chain alkoxycyanobiphenyl thiols indicating the capacitive behaviour of these monolayers with very less ionic permeation.

We have compared the ionic permeability of these SAMs of alkoxycyanobiphenyl thiols on Au surface obtained using the hexagonal liquid crystalline phase with that of the corresponding monolayers formed from dichloromethane as a solvent. Figure 26 shows the comparison of Bode phase angle plots of SAMs of C_5 (A), C_8 (B) and C_{10} (C) alkoxycyanobiphenyl thiols on Au surface formed from both the hexagonal liquid crystalline phase (b) and dichloromethane (a) as a solvating media. Insets show the corresponding Nyquist plots of the SAM modified electrodes in 1M NaF aqueous solution.

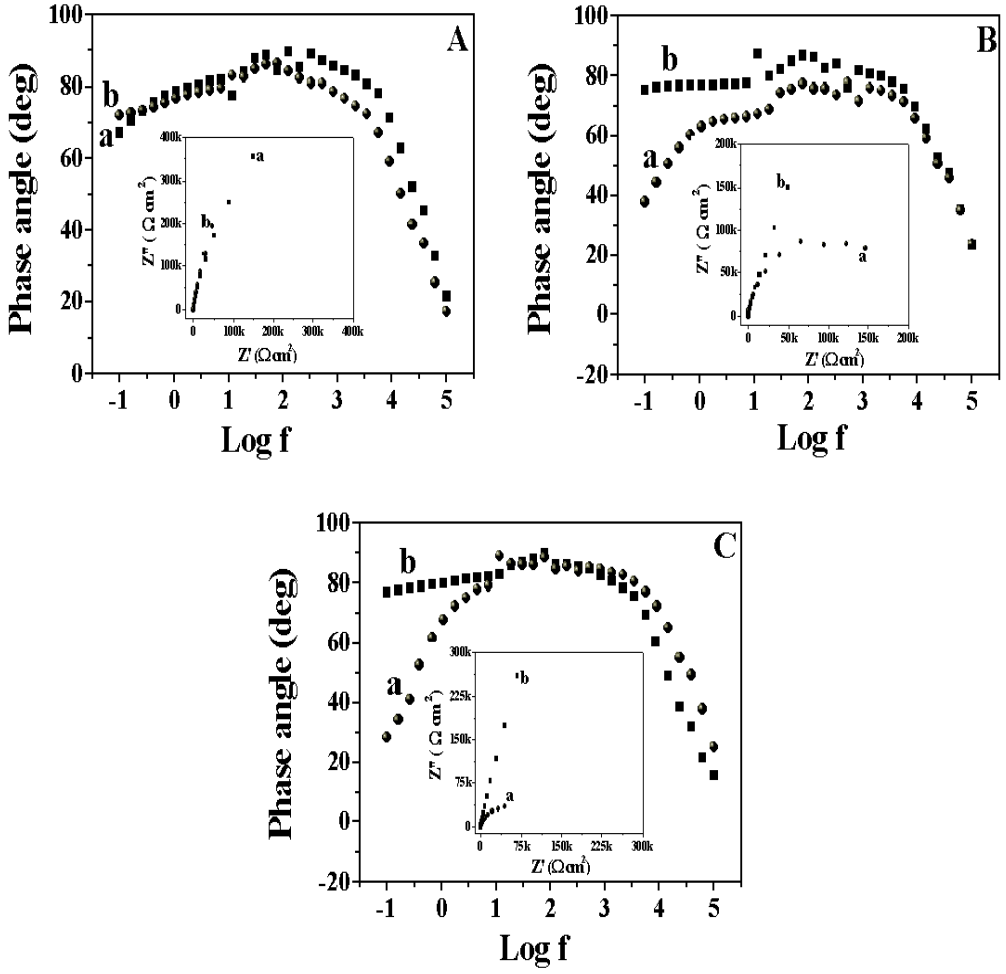

Figure 26: Bode phase angle plots in 1M NaF aqueous solution for the SAMs of C_5 (A), C_8 (B) and C_{10} (C) alkoxycyanobiphenyl thiols on gold surface obtained using both the hexagonal liquid crystalline phase (b) and dichloromethane (a) as solvating media. Insets show the corresponding Nyquist plots for the SAM modified electrodes obtained by keeping the Au strips in the thiol solution for about 15 hours.

It can be seen from the figures that the phase angle values of the monolayers formed from the hexagonal liquid crystalline phase (b) is higher than the one formed using dichloromethane (a) as a solvent. This effect is very clear especially in the cases of C_8 (B) and C_{10} (C) thiols on Au surface. The corresponding impedance values of the SAM modified electrodes are higher, as can be seen from the insets of the figure and the monolayers show an ideal capacitive behaviour when the hexagonal liquid crystalline phase is used as an adsorbing medium. From these figures, we also noted that the monolayers formed from dichloromethane by keeping the Au strips for long time is not good especially in the case of higher alkyl chain containing alkoxycyanobiphenyl thiols and this ultimately leads to a disorganization of the SAM by solvating the monolayer. This results in poor insulating properties of the SAMs as evidenced by the low phase angle and lower impedance values obtained in the case of C_8 (B) and C_{10} (C) thiols when dichloromethane is used as a solvent. These results are in conformity with our CV and impedance results discussed earlier. From these studies, we conclude that the SAMs obtained using the hexagonal liquid crystalline phase can be viewed as a pure capacitor with almost defect free structure and the SAMs formed from dichloromethane act as a leaky capacitor with the current path provided through the pinholes and defects in the monolayer. The higher phase angle obtained in the case of SAMs prepared from the hexagonal liquid crystalline phase even at lower frequencies, where ionic permeation is generally favoured, points out to the fact that a compact, dense monolayer has been formed with very low defects.

5.10. Proposed mechanism for the monolayer formation using the hexagonal liquid crystalline medium

Based on the experimental results obtained from the analysis of SAM modified electrodes using cyclic voltammetry and impedance spectroscopy measurements, we propose a plausible mechanism for the formation of monolayer and explain the better blocking ability of the SAMs prepared from the hexagonal liquid crystalline phase. The proposed mechanism is similar to that of the one reported for the formation of alkanethiolate SAMs from the aqueous micellar solution by Jennings et al. [30-33]. The formation of alkanethiolate SAMs from the hexagonal liquid crystalline phase is likely to involve several steps such as (a) the solubilization of thiol in the hydrophobic domains, (b) diffusion of thiol from the core to the gold surface, (c) delivery of thiol from the cylindrical rod either to the adsorbed cylindrical rod or directly to the gold surface and (d) nucleation of thiol domains on the Au surface and the replacement of physisorbed water molecules by the thiol molecules. In general, the use of solvents, which would weakly interact with the adsorbate (thiol) and provide less perturbation of van der Waals interchain interactions during self assembly process is preferred in order to form larger domains with fewer defects and grain boundaries. In our case, the use of hexagonal liquid crystalline phase provides a highly hydrophobic environment, which maximizes the solubilization of thiol. The use of aqueous medium eliminates the problem associated with the intercalation of solvent molecules thereby providing the way for better inter chain interactions of alkanethiols. It also overcomes the drawback usually associated with organic solvents such as their volatility and toxicity. The formation of homogeneous mixture of the hexagonal liquid crystalline phase after the addition of thiol implies a complete solubilization of thiol in the hexagonal liquid crystalline phase. These cylindrical rods containing

the thiol molecules orient laterally to the gold surface, which is the most probable orientation due to the hydrophilic nature of the gold surface and the polar nature of the molecules constituting the outside of the cylindrical rods. The thiol molecules encapsulated inside the core diffuses to the gold surface replacing the physically adsorbed water molecules. The cylindrical rods of the micelle depleted of water molecules are replenished by the freshly diffusing thiol molecules from the other micelles in the bulk. The proposed mechanism for the SAM formation is schematically depicted in figure 27.

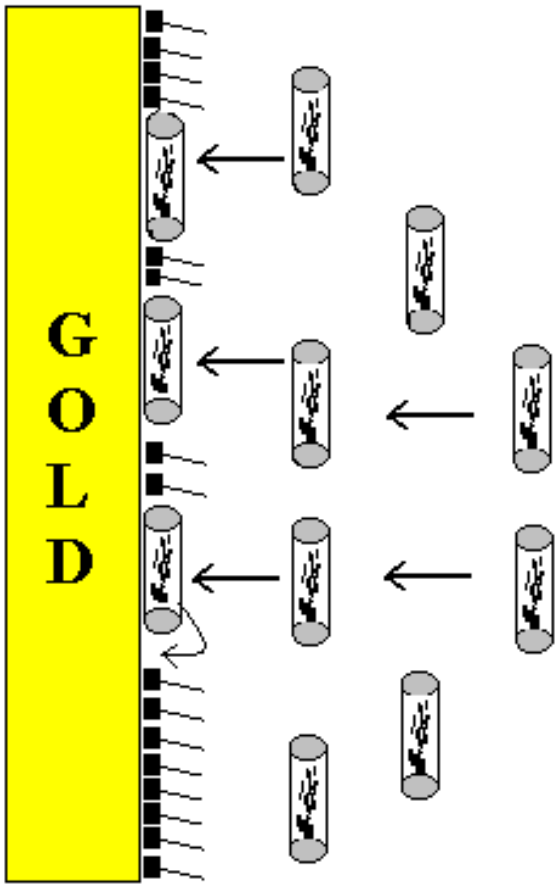

Figure 27: The schematic representation of the proposed mechanism for the better blocking ability of the monolayer prepared using the hexagonal liquid crystalline phase.

The very high surface coverage values of >99.98% obtained from the impedance spectroscopy measurements indicate the formation of larger domains of SAM on the Au surface with almost defect free structure. We feel that the process of monolayer organization is enhanced by the aqueous environment prevailing during adsorption in the hexagonal liquid crystalline medium. This is also confirmed by the early organization of the alkanethiol molecules discussed in the first section, which is reflected in the better blocking of the film to redox reactions, and ion permeation compared to the SAM prepared in organic solvents. The proposed mechanism explains the formation of compact, highly ordered, oriented monolayers from the hexagonal liquid crystalline phase in the cases of aliphatic and alkoxycyanobiphenyl thiols. In the case of aromatic thiols, the interaction between the thiol molecules and the liquid crystalline phase prevents the free delivery of thiol from the cylindrical rod to the Au surface, which ultimately results in poor SAM formation.

5.11. Conclusions

In this chapter, we have described a new method of preparing self-assembled monolayers (SAMs) on gold surface by using a lyotropic liquid crystalline phase as an adsorbing medium. We have studied and characterized the monolayer formation of some aliphatic thiols, aromatic thiols and alkoxycyanobiphenyl thiols having different alkyl chain lengths on Au surface using the hexagonal lyotropic liquid crystalline phase as an adsorbing medium. We have also compared our results with that of the corresponding SAMs prepared using organic solvents. The stability and blocking ability of these SAMs were characterized using grazing angle FTIR spectroscopy and electrochemical techniques such as cyclic voltammetry and electrochemical impedance spectroscopy. The lyotropic liquid crystalline medium possesses a

hexagonal structure consisting of a non-ionic surfactant Triton X-100, water and the corresponding thiol, which provides a highly hydrophobic environment to solubilize the thiols and later to facilitate their delivery to the gold surface. We find that the SAMs formed from the hexagonal liquid crystalline phase are highly compact and have excellent electrochemical blocking ability towards the redox probes than the conventional SAMs prepared from commonly used organic solvents such as ethanol and dichloromethane. However, this is not true in the case of aromatic thiols on Au surface, where the monolayer formed from organic solvents exhibits a better blocking property and insulating property than the one obtained using the hexagonal liquid crystalline phase.

The electrochemical techniques such as cyclic voltammetry and electrochemical impedance spectroscopy were extensively used to evaluate the blocking ability of these monolayers on Au surface. From the impedance studies, we have determined the capacitance of the monolayer-coated electrodes and the surface coverage of the SAM, which has been found to be >99.98% on gold surface. We have also estimated the extent of ionic permeability through the film and measured the rate constants for the redox reactions on the SAM modified electrodes. Our results show that the rate constants of $[Fe(CN)_6]^{3-|4-}$ and $[Ru(NH_3)_6]^{2+|3+}$ redox couples are very much lower in the case of monolayers of aliphatic and alkoxycyanobiphenyl thiols prepared in liquid crystalline phase when compared to the SAM formed in 1mM thiol in ethanol and dichloromethane solvents respectively, suggesting a better blocking ability of the SAMs in the former case. From the grazing angle FTIR spectroscopy studies, we have ruled out any co-adsorption of surfactant molecules on the Au surface. These results suggest that the SAMs of very low defect density and extremely low ionic permeability can be obtained when a hexagonal lyotropic liquid crystalline phase is used as an adsorbing medium. The use of aqueous

medium provides a route for the formation of a highly compact, dense monolayer with almost defect free structure, which is crucial in the applications and commercial development of devices based on SAM. This also eliminates several major problems associated with the organic solvents used for the preparation of monolayer. Based on the experimental results, we have proposed a possible mechanism for the monolayer formation on Au surface using the hexagonal liquid crystalline phase as an adsorbing medium.

References:

1. A. Ulman, *An Introduction to Ultrathin organic films from Langmuir-Blodgett to self-assembly*, Academic Press, San Diego, CA, (1991).
2. H.O. Finklea, *Self assembled Monolayers on Electrodes in Encyclopedia of Analytical Chemistry*, R.A. Meyers, Academic Press, John Wiley & Sons Ltd, Chichester.
3. H.O. Finklea, *Electrochemistry of organized monolayers of thiols and related molecules on electrodes: in Electroanalytical chemistry*, A.J. Bard, I. Rubinstein, (Eds.), Marcel Dekker, New York, (1996).
4. J.J. Hickman, D. Ofer, P.E. Laibinis, G.M. Whitesides, *Science*, 252, (1991), 688.
5. B.A. Cornell, V.L.B. Braach-Maksvytis, L.G. King, P.D.J. Osman, B. Raguse, L. Wieczorek, R.J. Pace, *Nature*, 387, (1997), 580.
6. I. Rubinstein, S. Steinberg, Y. Tor, A. Shanzer, J. Sagiv, *Nature*, 332, (1988), 426.
7. P.E. Laibinis, G.M. Whitesides, *J. Am. Chem. Soc.*, 114, (1992), 9022.
8. N. Ohno, J. Uehara, K. Aramaki, *J. Electrochem. Soc.*, 140, (1993), 2512.
9. T. Notoya, Q.W. Poling, *Corrosion*, 35, (1979), 193.
10. M.J. Tariov, D.R.F. Burgess, G. Gillen, *J. Am. Chem. Soc.*, 115, (1993), 5305.
11. E.W. Wollman, D. Kang, C.D. Frisbie, T.M. Larcovic, M.S. Wrighton, *J. Am. Chem. Soc.*, 116, (1994), 4395.
12. F.R.F. Fan, J.P. Yang, L.T. Cai, D.W. Price, S.M. Dirk, D.V. Kosynkin, Y.X. Yao, A.M. Rawlett, J.M. Tour, A.J. Bard, *J. Am. Chem. Soc.*, 124, (2002), 5550.

13. Y. Xiao, F. Patolsky, E. Katz, J.F. Hainfeld, I. Willner, *Science*, 299, (2003), 1877.
14. M. Aslam, N.K. Chaki, J. Sharma, K. Vijayamohanan, *Curr. Appl. Phys.*, 3, (2003), 115.
15. R. Haag, M.A. Rampi, R.E. Holmlin, G.M. Whitesides, *J. Am. Chem. Soc.*, 121, (1999), 7895.
16. Y. Kawanishi, T. Tamaki, M. Sakuragi, T. Seki, Y. Swuzki, K. Tchimura, *Langmuir*, 8, (1992), 2601.
17. H.I. Kim, M.B. Graupe, O. Oloba, T. Koini, S. Imaduddin, T.R. Lee, S.S. Perry, *Langmuir*, 15, (1999), 3179.
18. P.E. Laibinis, G.M. Whitesides, *J. Am. Chem. Soc.*, 114, (1992), 1990.
19. H.D. Sikes, J.F. Smalley, S.P. Dudek, A.R. Cook, M.D. Newton, C.E.D. Chidsey, S.W. Feldberg, *Science*, 291, (2001), 1519.
20. A. Ulman, *Chem. Rev.*, 96, (1996), 1533.
21. U.K. Sur, V. Lakshminarayanan, *J. Electroanal. Chem.*, 516, (2001), 31.
22. U.K. Sur, V. Lakshminarayanan, *J. Electroanal. Chem.*, 565, (2004), 343.
23. U.K. Sur, R. Subramanian, V. Lakshminarayanan, *J. Colloid Interface Sci.*, 266, (2003), 175.
24. R.P. Janek, R.W. Fawcett, A. Ulman, *Langmuir*, 14, (1998), 3011.
25. L.V. Protsailo, R.W. Fawcett, *Langmuir*, 18, (2002), 8933.
26. J. Israelachvili, *Intermolecular and Surface forces*, 2nd Ed., Academic Press, San Diego, CA, (1992).
27. A.N. Galatanu, I.S. Chronakis, D.F. Anghel, A. Khan, *Langmuir*, 16, (2000), 4922.
28. C. Miller, P. Cuendet, M. Gratzel, *J. Phys. Chem.*, 95, (1991), 877.
29. J. Liu, A.E. Kaifer, *Isr. J. Chem.*, 37, (1997), 235.
30. D. Yan, J.A. Saunders, G.K. Jennings, *Langmuir*, 16, (2000), 7562.

31. D. Yan, J.A. Saunders, G.K. Jennings, *Langmuir*, 19, (2003), 9290.
32. D. Yan, J.L. Jordan, V. Burapatana, G.K. Jennings, *Langmuir*, 19, (2003), 3357.
33. D. Yan, J.A. Saunders, G.K. Jennings, *Langmuir*, 18, (2002), 10202.
34. V. Ganesh, V. Lakshminarayanan, *Electrochim. Acta*, 49, (2004), 3561.
35. W.M. Gelbart, A. Ben-Shaul, D. Roux, (Eds.), *Micelles, Membranes, Microemulsions and Monolayers*, Springer-Verlag, New york, (1994).
36. S.V. Ahir, P.G. Petrov, E.M. Terentjev, *Langmuir*, 18, (2002), 9140.
37. M. Himmelhaus, F. Eisert, M. Buck, M. Grunze, *J. Phys. Chem. B*, 104, (2000), 576.
38. R. Subramanian, V. Lakshminarayanan, *Electrochim. Acta*, 45, (2000), 4501.
39. H.O. Finklea, D. Snider, J. Fedyk, E. Sabatani, Y. Gafni, I. Rubinstein, *Langmuir*, 9, (1993), 3660.
40. K. Tokuda, T. Gueshi, H. Matsuda, *J. Electroanal. Chem.*, 102, (1979), 41.
41. C. Amatore, J.M. Saveant, D.J. Tessler, *J. Electroanal. Chem.*, 147, (1983), 39.
42. E. Boubour, R.B. Lennox, *Langmuir*, 16, (2000), 4222.
43. E. Boubour, R.B. Lennox, *Langmuir*, 16, (2000), 7464.
44. E. Boubour, R.B. Lennox, *J. Phys. Chem. B*, 104, (2000), 9004.
45. S. Slawomir, P. Barbara, R. Bilewicz, *J. Phys. Chem. B*, 106, (2002), 5907.
46. S.M. Stole, M.D. Porter, *Langmuir*, 6, (1990), 1199.
47. M.D. Porter, T.B. Bright, D.L. Allara, C.E.D. Chidsey, *J. Am. Chem. Soc.*, 109, (1987), 3559.
48. R.G. Snyder, H.L. Strauss, C.A. Ellinger, *J. Phys. Chem.*, 86, (1982), 5145.
49. I.R. Hill, I.W. Levin, *J. Chem. Phys.*, 70, (1979), 842.
50. R.A. MacPhail, H.L. Strauss, R.G. Snyder, C.A. Ellinger, *J. Phys. Chem.*,

88, (1984), 334.

51. E. Sabatani, J. Cohen-Boulakia, M. Bruening, I. Rubinstein, *Langmuir*, 9, (1993), 2974.
52. A.W. Hayes, C. Shannon, *Langmuir*, 12, (1996), 3688.
53. M.A. Rampi, G.M. Whitesides, *Chem. Phys.*, 281, (2002), 373.
54. D.J. Wold, R. Haag, M.A. Rampi, C.D. Frisbie, *J. Phys. Chem. B*, 106, (2002), 2813.
55. P. Cyganik, M. Buck, W. Azzam, C. Woll, *J. Phys. Chem. B*, 108, (2004), 4989.
56. Y.T. Long, H.T. Rong, M. Buck, M. Grunze, *J. Electroanal. Chem.*, 524-525, (2002), 62.
57. J.F. Kang, A. Ulman, S. Liao, R. Jordan, *Langmuir*, 15, (1999), 2095.
58. H. Schonheer, F.J.B. Kremer, S. Kumar, J.A. Rego, H. Wolf, H. Ringsdorf, M. Jaschke, H. Butt, E. Bamberg, *J. Am. Chem. Soc.*, 118, (1996), 13051.
59. N. Boden, R.J. Bushby, P.S. Martin, S.D. Evans, R.W. Owens, D.A. Smith, *Langmuir*, 15, (1999), 3790.
60. R. Owens, D.A. Smith, *Mol. Cryst. Liq. Cryst.*, 329, (1999), 427.
61. H. Allinson, N. Boden, R.J. Bushby, S.D. Evans, P.S. Martin, *Mol. Cryst. Liq. Cryst.*, 303, (1997), 273.
62. Z.P. Yang, I. Engquist, J.M. Kauffmann, B. Liedberg, *Langmuir*, 12, (1996), 1704.
63. Y.T. Tao, M.T. Lee, *Thin Solid Films*, 244, (1994), 810.
64. S. Kumar, V. Lakshminarayanan, *Chem. Commun.*, (2004), 1600.
65. S.K. Pal, S. Kumar, *Liq. Cryst.*, 32, (2005), 659.
66. V. Ganesh, Santanu Kumar Pal, Sandeep Kumar, V. Lakshminarayanan, *J. Colloid Interface Sci.*, (2006), Article in press.